

POLITECNICO DI TORINO

Collegio di Ingegneria Meccanica, Aerospaziale, dell'Autoveicolo e della
Produzione

**Corso di Laurea Magistrale
in Automotive Engineering**

Tesi di Laurea Magistrale

EFFECT OF ELECTROMAGNETIC- SENSITIVE PARTICLES ADDITION ON REVERSIBILITY PERFORMANCES OF HOT-MELT ADHESIVES



Relatori

Prof. Giovanni Belingardi

Prof. Luca Goglio

Prof. Sayed Nassar

Candidato

Marco Attanasio

A.A. 2017/2018

Acknowledgements

I would like to express the deepest appreciation to my advisor at Oakland University, Dr. Sayed Nassar, for his full support, expert guidance, understanding and encouragement throughout my study and research.

I would like to thank my advisors at Politecnico di Torino, Prof. Giovanni Belingardi and Prof. Luca Goglio, that provided me their own expertise, insightful, and thoughtful comments and suggestions from overseas that have stimulated and improved my work.

Furthermore, I would like to thank all the team of Emabond Solutions™ for supporting this work and giving access to its technology center and the FCA Group for sponsoring this research work.

Thanks to all the colleagues and friends that I met in these two years in Turin and a special acknowledgment goes to Luca, Marco, Morgan and all the Windsor's guys. You became my American family in six months and this amazing experience would have not been the same without you.

Last but not least, my deep and sincere gratitude to my family for their continuous and unparalleled love. Thanks for giving me the opportunities that have made who I am encouraging me to explore new directions in life and to seek my goals always being next to me.

Abstract

In this research, the effect of electromagnetic-sensitive additives on the reversibility performance of Hot-Melt Adhesives (HMA), is studied. Test Single Lap Joints (SLJ) were made of Acrylonitrile Butadiene Styrene (ABS) adherends that were bonded using the modified thermoplastic HMA.

The heat produced by the interactions of a high-frequency electromagnetic field with the particles is used to bond the test joints. Particles of 2 sizes were added to the adhesive in 6 increasing weight percentages, up to 70 %. Variables such as process time, adhesive thickness and surface preparation were kept constant for all the specimens.

Tensile-shear tests at 2 different temperatures, before and after environmental exposure, and debonding tests were performed. A Dynamic Mechanical Analyzer (DMA) was used to characterize the adhesive with different levels of enrichment.

SLJ strength was found to be lower for moderate levels of adhesive enrichment, while it raised for higher weight percentages. Larger particle size and environmental cycling reduced considerably the static performances of the joints. Tests performed at 70 °C revealed a dramatic drop in Load Transfer Capacity (LTC), for both pristine and enriched adhesives.

Debonding tests showed that the time required for the joints disassembling shortens increasing the level of particles enrichment and particulate size, in accordance with what observed during the manufacturing process.

DMA results revealed that the particles enrichment does not modify the effect of temperature on the viscoelastic properties of the adhesive.

Sommario

In questo lavoro di ricerca è stato studiato l'effetto della dispersione di additivi magnetoreattivi di un Hot-Melt Adhesive (HMA). I Single Lap Joints (SLJ) testati sono stati realizzati con substrati di ABS incollati utilizzando un HMA termoplastico arricchito di particelle metalliche. Il calore prodotto dalle interazioni tra un campo elettromagnetico ad alta frequenza e le particelle è utilizzato per incollare i provini. Particelle di 2 dimensioni sono state aggiunte all'adesivo in 6 percentuali di massa crescenti, fino al 70 %. Variabili come il tempo di processo, lo spessore dell'adesivo e la preparazione dell'adesivo sono stati mantenuti costanti per tutti le configurazioni osservate.

Sono state effettuate prove di trazione a 2 diverse temperature, prima e dopo l'esposizione ad agenti atmosferici, e test di scollamento. Un Dynamic Mechanical Analyzer (DMA) è stato utilizzato per caratterizzare l'adesivo con diverse percentuali di particelle al suo interno.

È stata riscontrata una resistenza inferiore del giunto per valori medi di arricchimento, mentre essa è cresciuta per percentuali in massa maggiori. Una maggiore dimensione delle particelle e l'esposizione ad agenti atmosferici hanno ridotto notevolmente le prestazioni statiche del giunto. I test effettuati a 70 °C hanno rivelato un calo drastico nella Load Transfer Capacity (LTC), sia per l'adesivo originale che per quello modificato.

I test di scollamento hanno mostrato che il tempo richiesto per lo smontaggio del giunto si riduce incrementando il numero di particelle e la loro dimensione, concordando con quanto osservato durante la realizzazione dei giunti.

I test effettuati con la DMA hanno rivelato che l'aggiunta di particelle non modifica l'effetto della temperatura sulle proprietà viscoelastiche del materiale.

Table of contents

1	<i>Introduction and literature review</i>	<i>1</i>
1.1	Reversible adhesive bonding in automotive field	1
1.2	Hot-melt thermoplastic adhesives characterization	4
1.3	Metallic micro-particles addition	6
1.4	Single lap joint configuration	7
1.5	Research objectives	8
2	<i>Experimental procedure and test setup</i>	<i>10</i>
2.1	Room temperature tensile-shear tests	10
2.2	High temperature tensile-shear tests	13
2.3	Debonding tests	18
2.4	Adhesive characterization (DMA).....	22
3	<i>Preliminary tests</i>	<i>28</i>
3.1	Materials screening	28
3.2	Methodology	29
3.3	Preliminary results	31
4	<i>Manufacturing of test joints</i>	<i>41</i>
4.1	Material characteristics	41
4.2	Preparation of the particle-enriched adhesives	45
4.3	Assembling process	50

5	<i>Test data and discussions of results.....</i>	56
5.1	Quasi-static tensile-shear tests of Single Lap Joints.....	56
5.2	Reversibility performances	68
5.3	DMA tests	70
6	<i>Conclusions</i>	80
	Bibliography	82

List of Figures

Figure 1.1 - Single Lap Joint configuration	7
Figure 1.2 - ASTM D3163 – 01 - Single Lap Joint standard	8
Figure 2.1 - Hydraulic tensile test machine - MTS 810.....	11
Figure 2.2 - Thermotron Environmental Chamber	12
Figure 2.3 - Environmental cycle profile.....	13
Figure 2.4 - MTS Environmental chamber [19]	14
Figure 2.5 - FEA model – Single Lap Joint geometry	14
Figure 2.6 - FEA model - Particular of the mesh near bonding area	15
Figure 2.7 - FEA model - Sample temperature at the end of simulation	17
Figure 2.8 - FEA model - Adhesive temperature at the end of simulation	18
Figure 2.9 - L-shaped copper plate	19
Figure 2.10 - Debonding test - Single Lap Joint fixture.....	20
Figure 2.11 - Single Lap Joint for debonding tests.....	20
Figure 2.12 - Debonding tests - Setup	21
Figure 2.13 - TA Instruments Q800 Dynamic Mechanical Analyzer (DMA) [23]	22
Figure 2.14 - Response of viscoelastic materials to a sinusoidal oscillation	24
Figure 2.15 - DMA Thin-film tension clamp [25]	25
Figure 2.16 - DMA test setup – Adhesive sample with 60 % of small particles	26
Figure 2.17 - DMA test setup - Pristine Hot-Melt adhesive	27
Figure 3.1 - Interfacial failure mode - PC/ABS substrate with Admer NE827	32
Figure 3.2 - Load vs. Displacement curve - PC/ABS substrate with Admer NE827.....	32
Figure 3.3 - Interfacial failure mode - Nylon 6 substrate with Admer QF500T	33

Figure 3.4 - Load vs. Displacement curve - Nylon 6 substrate with Admer QF500T	33
Figure 3.5 - Interfacial failure mode - HDPE substrate with Admer QF551T.....	34
Figure 3.6 - Load vs. Displacement curve - HDPE substrate with Admer QF551T	34
Figure 3.7 - Interfacial failure mode - Nylon 6 substrate with Dow GR 204.....	35
Figure 3.8 - Load vs. Displacement curve - Nylon 6 substrate with Dow GR 204	35
Figure 3.9 - Interfacial failure mode - PC/ABS substrate with Bostik TG 9446.....	36
Figure 3.10 - Load vs. Displacement curve - PC/ABS substrate with Bostik TG 9446....	36
Figure 3.11 - Interfacial failure mode - ABS substrate with Bostik Thermelt 865	37
Figure 3.12 - Load vs. Displacement curve - ABS substrate with Bostik Thermelt 865..	37
Figure 3.13 - Interfacial failure mode - ABS substrate with Ellsworth AP-122 H.....	38
Figure 3.14 - Load vs. Displacement curve - ABS substrate with Ellsworth AP-122 H ..	38
Figure 4.1 - Pristine HMA in pellets	42
Figure 4.2 - Iron particles sizes - Smaller (left) and bigger (right)	43
Figure 4.3 - Profilometer analysis - ABS substrate with no surface treatment	44
Figure 4.4 - Adhesive enrichment - Equipment.....	45
Figure 4.5 - Oven	46
Figure 4.6 - Pressing machine	48
Figure 4.7 - Adhesive sheets - Baseline (a), 30 % (b) and 60 % (c) big particles	49
Figure 4.8 - Optical microscope scanning, 50x magnification - HMAs with 20 % of small (left) and big (right) iron particles	49
Figure 4.9 - Optical microscope scanning, 50x magnification - HMAs with 70 % of small (left) and big (right) iron particles	50
Figure 4.10 - CAD Scheme of the coil.....	51
Figure 4.11 - CAD Scheme of the bonding machine	52
Figure 4.12 - Path of melting process	53

Figure 4.13 - Bonding process - Time evaluation with LCR Thermometer	53
Figure 4.14 - Time to complete bonding process	54
Figure 5.1 - Effect of particulate size - Room Temperature Baseline	56
Figure 5.2 - Load vs. Displacement curve - HMA with 20 % of smaller iron particles...	58
Figure 5.3 - Load vs. Displacement curve - HMA with 70 % of smaller iron particles...	59
Figure 5.4 - Interfacial failure mode - Room Temperature with 20 % (left) and 70 % (right) of “big” iron particles.....	59
Figure 5.5 - Effect of particulate size - Room Temperature after env. cycling	60
Figure 5.6 - Effect of environmental cycle - Room Temperature - Small particles	61
Figure 5.7 - Effect of environmental cycle - Room Temperature - Big particles	62
Figure 5.8 - Interfacial failure mode - Room Temperature after environmental cycle with 20 % (left) and 70 % (right) of “big” iron particles.....	62
Figure 5.9 - Effect of particulate size - High Temperature Baseline	64
Figure 5.10 - Effect of particulate size - High Temperature after env. cycling	64
Figure 5.11 - Effect of environmental cycle - High Temperature - Small particles	65
Figure 5.12 - Effect of environmental cycle - High Temperature - Big particles	65
Figure 5.13 - Effect of testing temperature - Baseline - Small particles.....	66
Figure 5.14 - Effect of testing temperature - Cycled Small particles	67
Figure 5.15 - Interfacial failure mode - High Temperature with 20 % (left) and 70 % (right) of “big” particles.....	67
Figure 5.16 - Time required to debond the Single Lap Joints.....	68
Figure 5.17 - Storage modulus - Effect of weight percentage - Frequency of 1 Hz.....	71
Figure 5.18 - Storage modulus - Effect of particulate size (60 % enrichment) - Frequency of 1 Hz.....	72

Figure 5.19 - Storage modulus - Effect of frequency - Adhesive with 60 % of smaller particles	73
Figure 5.20 - Loss modulus - Effect of particles weight percentage - Frequency of 1 Hz	74
Figure 5.21 - Loss modulus - Effect of particulate size (60 % enrichment) - Frequency of 1 Hz	75
Figure 5.22 - Loss modulus - Effect of frequency - Adhesive with 60 % of small particles	75
Figure 5.23 - Tan Delta - Effect of adhesive enrichment - Frequency of 1 Hz	76
Figure 5.24 - Quasi-static tensile test - Effect of testing temperature - Pristine adhesive	77
Figure 5.25 - Quasi-static tensile test - Effect of enrichment level - Room Temperature	78
Figure 5.26 - Quasi-static tensile test - Effect of particulate size - Room Temperature..	79

List of Tables

Table 2.1 - Air properties @ 70 °C [20]	16
Table 2.2 - Hot-Melt Adhesive properties [21]	16
Table 2.3 - Average ABS properties [22]	16
Table 3.1 - List of the Adhesives	28
Table 3.2 - List of the Substrates	29
Table 3.3 - Preliminary results recap	31
Table 3.4 - Lap Shear Strength - ABS with Bostik Thermelt 865	40
Table 4.1 - Adhesive characteristics [26]	42
Table 4.2 - Iron particles dimensions	43
Table 4.3 - ABS Lustran 433 Technical data [27]	44
Table 4.4 - Mass of compound required for pressing phase	47

1 Introduction and literature review

Adhesive bonding is now extensively considered to be the replacement of conventional joining methods such as riveting, bolting and welding being able to maintain mechanical properties and durability, also in structural applications. The automotive industry is facing challenges of implementing recyclable polymeric materials on vehicle structures. Traditional joining techniques show drawbacks in these types of application either adding extra weight to the structure or creating inefficient joints when dissimilar materials are adopted.

Laws on recyclability represent the main issue for the application of adhesive joints. Due to this fact, it is essential to obtain a solution that guarantees excellent structural solutions in terms of fatigue and impact strength and that can allow an easy disassembling and recycling process.

1.1 Reversible adhesive bonding in automotive field

In principle, adhesive joints are structurally more efficient than mechanically fastened or welded joints because they reduce stress concentrations present in holes or welding lines. Adhesives could have a higher resistance to environmental factors [1] and they are usually preferred to traditional fasteners when joining components made of different materials [2, 3]. Moreover, they offer the possibility of joining hybrid structures, that are the most promising way to obtain lightweight vehicle design.

Nowadays, car manufacturers are designing their vehicles increasingly lighter with the objective of reducing both fuel consumption and the environmental pollution. In the European Union, the limits on CO₂ emissions have been continuously reduced and every new car will satisfy the limit of 95 g/km of CO₂ emissions within 2021. In this scenario, multi-material

structures and adhesives can offer a big contribution to the design of lightweight vehicles [4]. The demand for lower emissions and the necessity to improve fuel economy in passenger vehicles are the driving forces behind the increasing request for lightweight materials in the automotive field.

As Lu et al. [5] have observed, the main drivers for change are the international legislations on End-of-Life Vehicles together with the demand and the including future supply of materials. In the European Union, the directive 2000/53/EC has as its main objective the prevention of waste from vehicles and, in addition, the reuse or other forms of recovery of ELVs and their components. Therefore, manufacturers have to build vehicles with a design that aims to increase recoverability of as much parts as possible. This regulation is active from January 2015 and declares that all ELVs must have a recovery rate of 95 % and a recycling rate of 85 % by an average weight per vehicle and year.

In previous years, thermosetting polymers have been preferred to other adhesives in order to create stiff and strong structural adhesive joints, as they guarantee higher strength and elastic modulus. However, in recent decades, the use of thermoplastic adhesives has been considered and progressively increased in the automotive industry as well. At the beginning, they have been applied for non-structural applications and then for some structural one [6].

The most widely adopted solution is represented by the adoption of hot-melt thermoplastic adhesives exploiting their nature of reversibility at high temperature. Nowadays, they are used both for components inside the passenger compartment and for exterior parts. Typical bonded interior components are plastic components such as trim, instrument panel, ducts and pipes for the air conditioning system and many other applications that require the fastening of non-structural plastic, wooden or fabric parts. For the exterior components, the harsh environment imposes that the adhesives have to overcome to the exposure to severe conditions and, in some

cases, also relatively high loading conditions. Typical exterior applications for HMAs are plastic bumpers, doors, plates, lamps, lamp housings, skirts and glass roofs [6].

Thermoplastic HMAs allow joining solutions for dissimilar materials thus overcoming the limits of welded and bolted joints in terms of weight and hybrid joining. However, as Verna et al. [7] and Banea et al. [8] have observed, problems arise when bonds have to be broken without damage of the components. Currently, debonding of structural adhesive joints is mainly based on mechanical destruction. This process can damage or even destroy the substrates, making recycling complex or impossible.

The reversibility nature of hot-melt thermoplastic adhesives is limited by the huge amount of energy required to melt the adhesive. In fact, the needed heat may damage the substrates if they are made of plastic with a melting temperature that usually is close to the one of the HMA itself. This issue is overcome by inserting susceptible micro- or nano-particles inside the baseline adhesive polymer matrix.

The physics of electromagnetic induction applies to both Joule heating and magnetic heating. Benatar [9] has described the heating of ferromagnetic susceptor materials as the combinations of both these effects. Nanoparticles are being used in automotive industries to foreshorten the curing time of thermosetting adhesives. For instance, the curing time of a commercially available epoxy-based adhesive is in the range of several hours. However, with embedded susceptible particles inside, when subjected to electromagnetic field, its curing time is reduced to around 17 min. The results depend on the power generated by the induction coil that generates eddy current around the matrix modified with nanoparticles, by their weight percentage in the polymer matrix and by the permissibility value that characterizes the considered particle type. Appropriate controlled power should be supplied to avoid material degradation because of too high temperature [7].

1.2 Hot-melt thermoplastic adhesives characterization

Hot-melt adhesives represent the only feasible solution for reversible adhesive joints at the moment. They have been widely recognized in different engineering fields such as aeronautic, naval, etc. to join non-structural components. HMAs are a one-component system which consists of a non-volatile thermoplastic polymer which is solid at room temperature, has fluid characteristics while in the molten state and solidifies quickly when allowed to cool down [10].

The drawbacks for such a system are the limited adhesive strength achieved, and the lack of molten properties such as tack and wetting ability which directly affect the performance of the hot-melt adhesive. In actual situations, the composition of a hot-melt adhesive usually includes a thermoplastic polymer backbone and a diluent system.

Since hot-melt adhesives need to be applied in the molten state, polymers with adequate resistance to heat degradation such as polyethylene, polyvinyl acetate or ethylene-vinyl acetate copolymers are typically used as the backbone polymer. Moreover, high molecular weight polymers are preferred since they provide high viscosity, high (cohesive) strength and good mechanical properties [11]. The diluent system in a hot-melt adhesive can include materials such as wax, tackifier and plasticizer. By adding these materials accordingly, the properties of the HMAs can be modified and customized to a specific end usage [12]. The diluent system can help to lower the viscosity of the molten polymer making it more convenient to apply onto surfaces as well as to increase the wetting ability and adhesive strength.

Hot-melt adhesives are solvent-free, a selling point which increases their desirability in potential markets due to the lower health risks associated with using these products. Another advantage is that they have a simple bonding mechanism at a fairly high bonding rate once

applied. Besides, those kinds of adhesives are ideal for maintenance of plastic components such as internal or external trims of vehicles.

HMAs are also cleans and easy to automate. Since hot-melt adhesives are usually water-insoluble, they can be used as a joining means and a gap filler in many applications. In particular, in automotive and appliance industries they are extensively utilized to bond a wide variety of porous and non-porous substrates including pre-painted steel and polyolefin plastics, with low to no toxicity. However, hot-melt adhesives exhibit lower strength and heat resistance compared to conventional thermosetting adhesives such as epoxies or cyanoacrylate because they are thermoplastic materials that cannot react or cure to form crosslinks. [12]

Due to short cure time and their environmentally friendly nature, HMAs raw material formulations have been continuously improved to allow adhesive manufacturers to engineer new high-performance adhesives. Raw materials include tack resins, waxes, antioxidants, plasticizers and other fillers which are incorporated into base hot-melt resins to enhance adhesive performance. For instance, natural or synthetic tackifiers are generally added to certain formulations to improve the adhesion, surface wetting, open time, polymer flexibility or tack of the adhesive. Waxes help diminish pellet blocking, reduce melt viscosity, and/or modify the tack or “green strength” of the adhesive. Antioxidants are used to prevent the resin from oxidizing and to aid in processing and storage tank stability of large volumes [13].

Today’s high performance structural hot melts, formulated with advanced raw materials, include ethyl vinyl acetate (EVA) adhesives for general purpose bonding, polyolefin adhesives for difficult-to-bond plastics, polyamide adhesives for severe environments, and reactive urethanes for elevated temperature or high flexibility requirements.

1.3 Metallic micro-particles addition

One of the critical problems linked to adhesive joint in automotive application is that it does not allow disassembling components during maintenance and recycling processes. Due to continuous rising in demand of implementation of recyclable thermoplastic materials on vehicle structures, appropriate joining techniques are essential to facilitate easy of disassembly and to optimize the recycling process [12].

Hot-melt thermoplastics adhesives represent one of the promising solutions thanks to their environmentally friendly nature and affordable price. By taking into consideration their property of being reversible at high temperature, studies have been done on selected HMAs and thermoplastic substrate materials to investigate the effect of metallic nano-particles embedded inside those polymer matrixes when electromagnetic field is emitted around them.

Due to the existence of many mobile electrons, which leads to a heat transfer into the surrounding matrix by friction losses, metallic nano-particles efficiently generate heat in the presence of electromagnetic field. They may induce phase transformation when they are in thermal contact with a polymer or a solid matrix [14].

In medical field, a lot of research activities have been done on functional enhancement of polymeric and other of matrixes such as ice, by utilizing metallic nano-particles. [15, 16 & 17] use nano-particles to release materials from a polymer capsule containing Au nano-particles excited with intense light that are destroyed as a result of heating effect.

On the other hand, nano-particles are being used in automotive industries to foreshorten the curing time of thermosetting adhesives and ultimately to achieve comparatively minimum assembly time. The curing time is dependent on the power generated by the induction coil that generates the eddy current around the matrix modified with metallic nano-particles, by the

amount of weight of the particles in the matrix and by their permissibility. With a controlled mixing mechanism, nano-particles play a great role towards an improved mechanics and rheological control.

1.4 Single lap joint configuration

Mechanical tests have been carried out on the configuration of the Single Lap Joint (SLJ) whose geometry is shown in the figure 1.1.

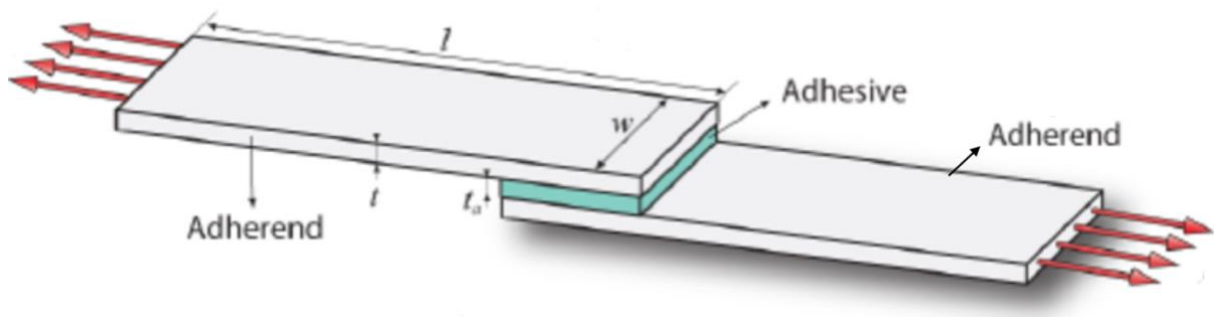


Figure 1.1 - Single Lap Joint configuration

The SLJ represents one of the most studied bonded joints in research and industries due to its easy assembly procedure and because the lap shear strength is a useful parameter for adhesive strength evaluation.

The tests that have been carried out in the second and main part of this study follow the ASTM D3163 – 01 standard [18] that defines simple rules to design the size of the substrates, the speed of the cross head, the adhesive overlap and the adhesive thickness to determine the strength of adhesively bonded rigid plastic lap-shear joints in shear by tension loading.

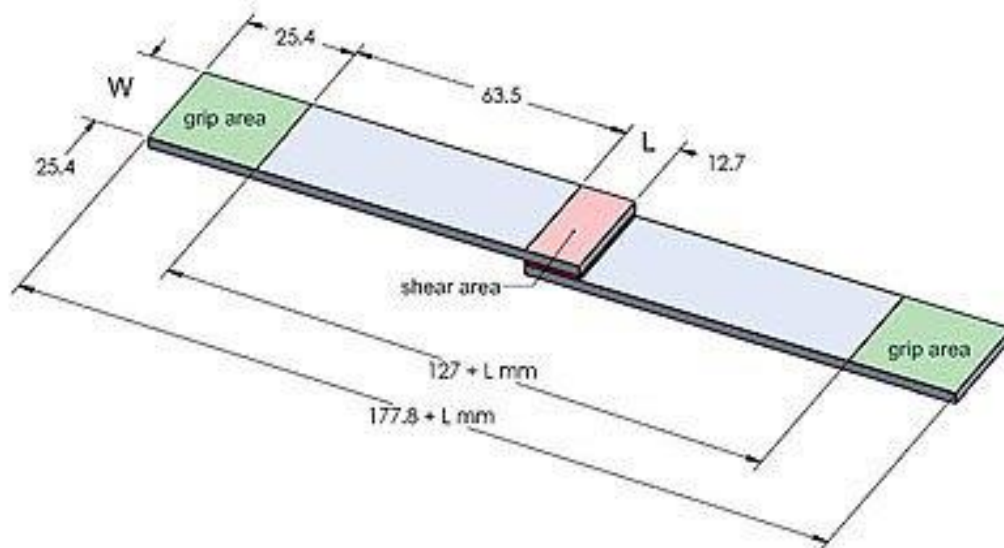


Figure 1.2 - ASTM D3163 – 01 - Single Lap Joint standard

1.5 Research objectives

The objective of this work is the study of the effects of the weight percentage and size of the particles that are embedded in the adhesive matrix in terms of LTC and debonding time. The idea behind this research is the need of the industrial world to find a feasible solution of modified hot-melt adhesive application in terms of time required for assembling and disassembling the parts and of strength performance of the bonded substrates. To this purpose, a slightly different path has been followed with respect to other previous research works. In previous works [7, 8 & 12], it has been observed the behavior of modified adhesives with up to 20 % of particles addition. On the other hand, the focus of this thesis is on HMAs with an addition of weight percentages of iron particles up to 70 % in order to increase heat transfers and, therefore, reduce the time required to join parts to values that are feasible for industrial time frames.

This work is divided in two main parts. In a first preliminary phase, seven different adhesives have been tested with eight types of substrates. The tests are focused on evaluating the best combination adhesive-adherend to proceed this work with in terms of load transfer capacity. All the samples have been tested at room temperature with shear tests on single lap joint configurations.

The second part of this thesis concentrates on the study of the effect of the weight percentage and size of the particles embedded in the polymer matrix. Iron particles of two dimensions have been added to the baseline adhesive selected from the first part of the tests in weight percentages of 20 %, 30 %, 40 %, 50 %, 60 % and 70 %.

The different 12 combinations of samples have been tested with shear tests on single lap joint configurations at room temperature and at a temperature of 70 °C. Half of the samples have been tested right after being subjected to a cycle at controlled temperature and humidity in an environmental chamber.

In order to evaluate the performances in terms of debonding time, all the combinations of samples have been subjected to disassembly tests in order to evaluate the time required to debond the specimen.

2 Experimental procedure and test setup

This study aims at evaluating the effects of the weight percentage and of the size of the susceptible particles embedded in the polymer matrix of a hot-melt thermoplastic adhesive in terms of strength and reversibility performances.

Shear tests have been performed on the SLJs at room temperature and at 70 °C. Half of the tested samples have been subjected to a temperature-humidity controlled cycle to observe the effects on the load transfer capacity of the joint due to environmental factors.

Debonding tests have been performed to evaluate the time required to disassemble the joint at room temperature.

Later, a more detailed characterization of the adhesive has been done by using the Dynamic Mechanical Analysis machine with dynamic and quasi-static tensile tests.

2.1 Room temperature tensile-shear tests

Quasi-static shear tests have been performed according to the ASTM D3163 standard with a hydraulic tensile test machine produced by MTS. An axial load has been applied at a constant speed of 0.5 in/min (1.27 mm/min). Each end of the specimen has been engaged to the grippers for a length of 1 in (2.54 mm) with a grip pressure of 0.5 bar. Rectangular spacers of polycarbonate with a thickness of 1/8 in (3.125 mm) have been inserted in the grippers in order to reduce the bending effect during the shear tests.



Figure 2.1 - Hydraulic tensile test machine - MTS 810

Tests have been done at room temperature and at a temperature of 70 °C. Three test repetitions have been performed for each combination of adherend-adhesive that has been considered.

Data have been recorded and load vs displacement curves have been generated to obtain informations about the load transfer capacity, which is the maximum load that each single-lap joint is able to sustain. The results on the LTC have been averaged on the overlap area which is nominally 0.5 in² (322.58 mm²) but has been precisely measured for each sample.

Half of the manufactured specimens have been subjected to a temperature-humidity controlled environmental cycle in a Termotron Environmental Chamber.



Figure 2.2 - Thermotron Environmental Chamber

The adopted environmental cycle simulates the conditions in which the observed materials may be subjected in real life applications. The relative humidity is fixed to a constant value of 80 % throughout all the cycle. The temperature oscillates between 20 °C and 70 °C with the following the profile illustrated in the Fig. 2.2. The cycle is repeated 12 times to an overall duration of 72 hours.

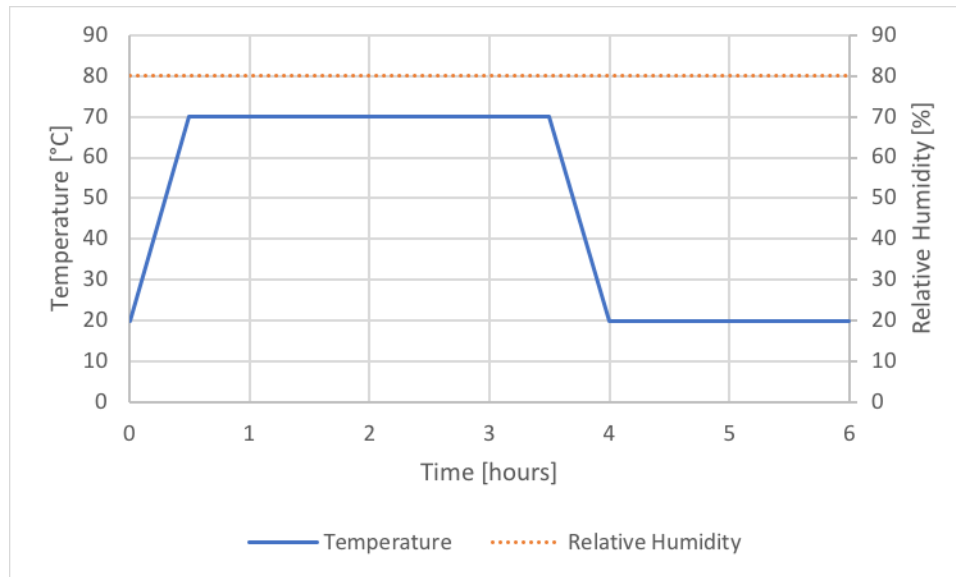


Figure 2.3 - Environmental cycle profile

Each environmental cycle has started 3 hours after the manufacturing of the corresponding joints. The samples subjected to the cycle have been tested with the MTS machine 15 hours after the ending of the cycle. The other specimens have been tested 15 hours after their manufacturing.

2.2 High temperature tensile-shear tests

Quasi-static shear tests have been performed at a temperature of 70 °C in order to understand the effects of the temperature on the strength performances of the joint in terms of LTC. To this purpose, the samples have been placed in the hydraulic tensile machine previously surrounded by the environmental chamber provided by MTS. A ceramic fiber insulation having thickness of 1 in (25.4 mm) has been inserted between the walls of the environmental chamber and the hydraulic cylinders of the MTS tensile machine to avoid dispersion of the heat generated in the chamber.



Figure 2.4 - MTS Environmental chamber [19]

A FEM model has been developed with the software ABAQUS to have a guideline about the time required to obtain a uniform temperature of 70 °C for the system comprising the machine itself, the air inside the chamber and the sample gripped to the MTS machine.

A customized mesh has been developed for the single lap joint to observe the effect of the heat transfer by conduction and convection.

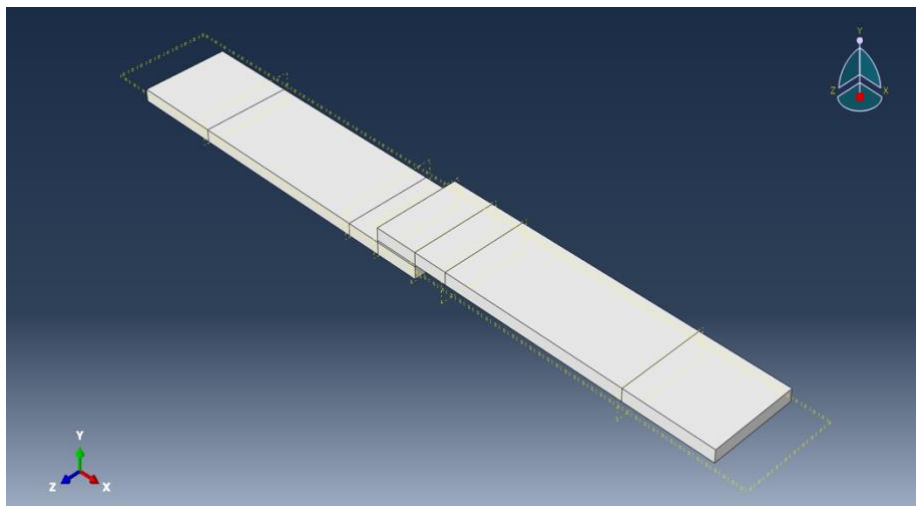


Figure 2.5 - FEA model – Single Lap Joint geometry

In particular, a more refined mesh has been created in the proximity of the overlap area and in the overlap area itself to obtain more accurate results in terms of heat transfer from the air to the substrates and then to the adhesive sheet.

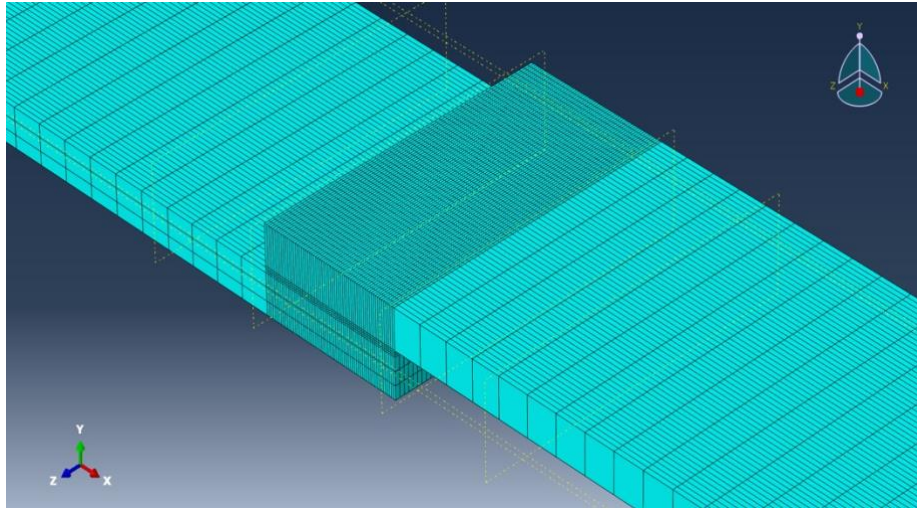


Figure 2.6 - FEA model - Particular of the mesh near bonding area

It has been assumed that the SLJ was submerged in a region in which air flows at a constant speed of 1 m/s and direction perpendicular from the side surface of the joint. Forced convection has been imposed on all the substrate walls with the exception of the side surface that is located further from the air flow source. In fact, it has been considered negligible the effect of air flow in the rear part of the chamber close to the sample in which a depression area is created by the presence of the SLJ and only natural convection may be observed. On the other hand, conduction has been imposed between the substrates and the adhesive and between the machine and the substrates in the areas in which the specimen is gripped to the MTS machine.

In the following tables the data inserted in the model for the air, the adhesive and the substrates are provided.

Table 2.1 - Air properties @ 70 °C [20]

Temperature [°C]	T_{air}	70
Speed [m/s]	U_{air}	1
Viscosity [Pa·s · 10 ⁻⁶]	μ_{air}	20.44
Density [Kg/m ³]	ρ_{air}	1.029
Specific Heat [J/(Kg·K)]	c_{air}	1.009
Thermal Conductivity [W/(m·K) · 10 ⁻³]	k_{air}	24.35

Table 2.2 - Hot-Melt Adhesive properties [21]

Thermal Conductivity [W/(m·K)]	$k_{adhesive}$	0.259
Specific Heat [J/(Kg·K)]	$c_{adhesive}$	1800

Table 2.3 - Average ABS properties [22]

Thermal Conductivity [W/m·K]	k_{sub}	0.18
Specific Heat [J/(Kg·K)]	c_{sub}	1423.5

The heat transfer coefficient h has been calculated starting from the given data and having evaluated the Reynolds, Prandtl and Nusselt coefficients.

The Reynolds number has been obtained by solving the equation (1) in which L is the characteristic length of the considered geometry that has been imposed to 0.0254 m, equal to the width of the SLJ.

$$Re = \frac{\rho_{air} \cdot U_{air} \cdot L}{\mu_{air}} = 1279 \quad (1)$$

The Prandtl number has been calculated using the formula (2).

$$Pr = \frac{\mu_{air} \cdot c_{air}}{k_{air}} = 0.847 \quad (2)$$

The obtained Reynolds number falls in the laminar region and the Prandtl number has a value bigger than 0.6. These results have allowed to obtain the average Nusselt number for a laminar flow on a flat plate using the formula (3).

$$\overline{Nu} = 0.664 \cdot Re^{1/2} \cdot Pr^{1/3} \quad (3)$$

The Nusselt number is defined by the equation (4):

$$Nu = \frac{h \cdot L}{k_{air}} \quad (4)$$

Therefore, the heat transfer coefficient h has been evaluated and set into the FEM model with a value of 21.539 W/m²K.

The ΔT between initial and final temperature of the simulation has been set to a value of 45 °C considering the starting point of the run at a temperature of 25 °C.

The results of the simulation have shown that a uniform temperature of 70 °C is reached in both substrates and adhesives after 871 s as shown in the Fig. 2.7 and 2.8.

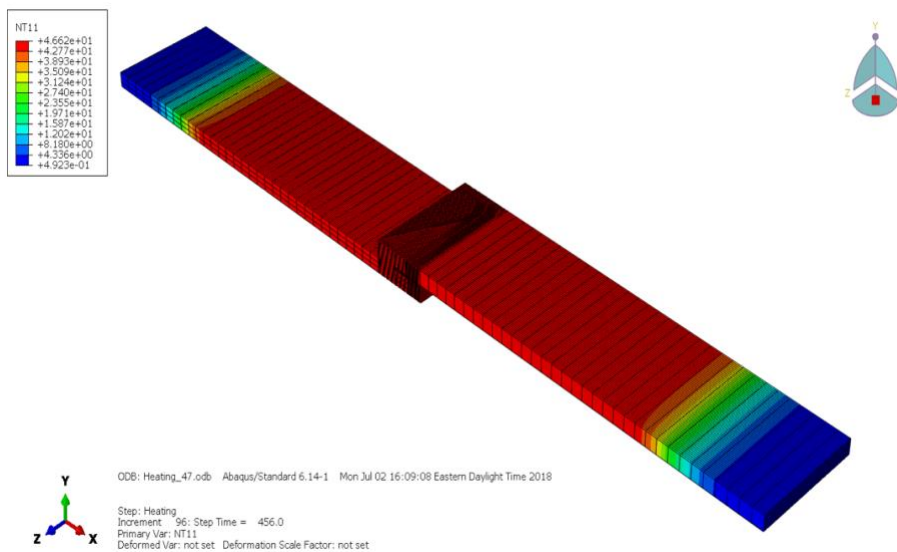


Figure 2.7 - FEA model - Sample temperature at the end of simulation

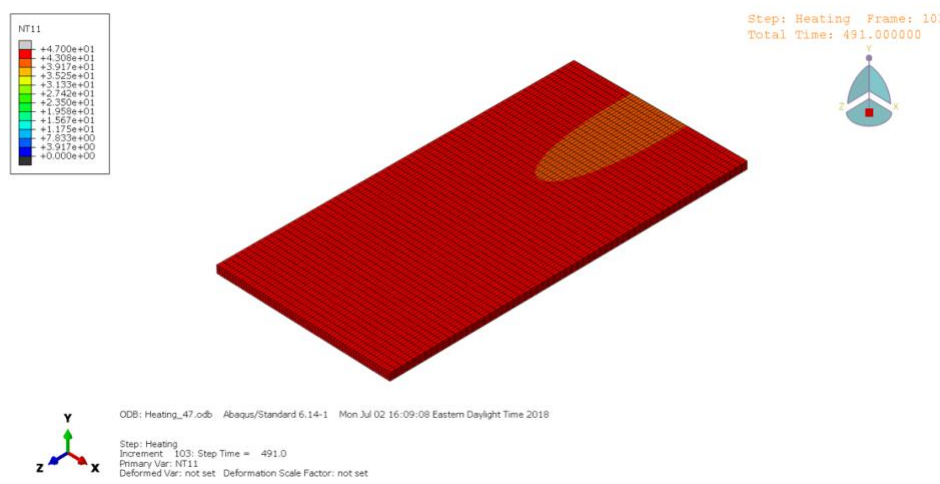


Figure 2.8 - FEA model - Adhesive temperature at the end of simulation

Given these approximated results from the FEM model, a similar methodology has been chosen for the experimental tests. Each sample has been positioned in the MTS environmental chamber with one of the two halves of the joint left free to move to avoid any type of compression stress due to linear elongation of the material due to the increasing temperature. The environmental chamber has been closed and activated with a temperature ramp of 30 °C/min. After the reaching of the temperature of 70 °C, the sample has been kept at constant temperature in the chamber for 15 minutes according to the results of the FEM simulation. Then, also the second half of the joint has been blocked in the grippers of the MTS machine with a grip pressure of 0.5 bar. The shear tests have been performed with the same methodology described in the paragraph 2.1 related to the quasi-static shear tests at room temperature.

2.3 Debonding tests

One of the main objectives of this study is represented by the possibility of disassembling joints exploiting the presence of metal susceptible particles inside the matrix of a thermoplastic

adhesive in order to make possible the repair and substitution of components without the need of destroying mechanically the bond that may cause damages to the parts themselves.

To this purpose, debonding tests have been performed on samples realized with the same methodology that has been adopted for the specimens used for the shear tests. Three experiments have been performed for each configuration of the modified hot-melt adhesives.

The setup of these experiments follows the one that has been adopted in previous works present in the literature [7, 8]. Holes have been drilled in the substrates in order to connect them to a weight having mass of 500 g by means of a twine. The same equipment that was used to assemble the joints, has been used for these debonding tests. The only modification that has been done to the system is represented by a new positioning of the coil in vertical position. This has been realized interposing the L-shaped copper plate showed in Fig. 2.9 between the coil and the plate connected to the capacitors of the machine.

The other half of the specimen has been fixed to the coil with a temperature resistant tape. The full configuration for the debonding test is shown in the Fig. 2.12.



Figure 2.9 - L-shaped copper plate



Figure 2.10 - Debonding test - Single Lap Joint fixture



Figure 2.11 - Single Lap Joint for debonding tests

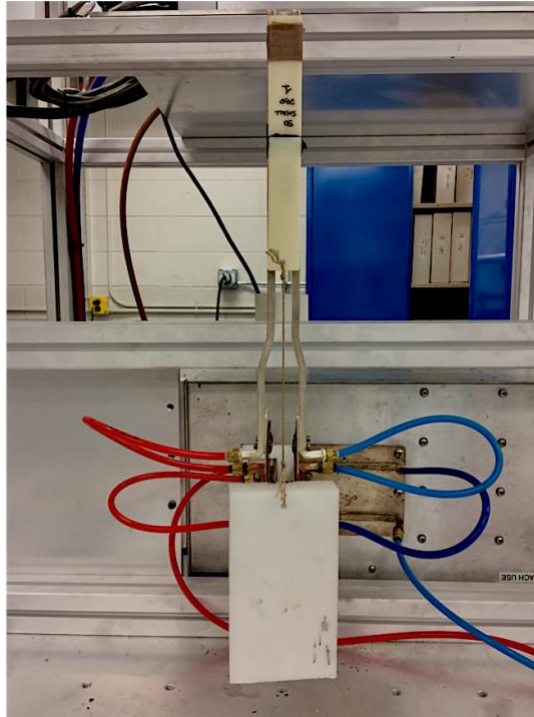


Figure 2.12 - Debonding tests - Setup

The controller of the machine has been set to the same configuration utilized for the bonding process with a power of 500 W.

The tests have been considered as finished at the time instant in which the weight connected to the joint reached the floor of the machine after a fully disassembly of the SLJ. The process time has been measured with the controller of the machine itself. Three test repetitions have been performed for each combination of weight percentage and size of the metal particles that has been investigated in this study for a total amount of 36 tests.

2.4 Adhesive characterization (DMA)



Figure 2.13 - TA Instruments Q800 Dynamic Mechanical Analyzer (DMA) [23]

The Dynamic Mechanical Analysis (DMA) is a thermal analysis technique that measures the properties of materials as they are deformed under periodic stress. In particular, a variable sinusoidal strain is applied, and the resultant sinusoidal stress is measured. If the material being evaluated is purely elastic, the phase difference between the stress and strain sine waves is 0° (i.e. they are in phase). If the material is purely viscous, the phase difference is 90° . However, most real-world materials including polymers are viscoelastic and exhibit a phase difference between those extremes. This phase difference, together with the amplitudes of the stress and strain sine waves, is used to determine a variety of fundamental material parameters, including storage and loss modulus, $\tan \delta$, complex and dynamic viscosity, transition temperatures, creep,

and stress relaxation, as well as related performance attributes such as rate and degree of cure, sound absorption, impact resistance and morphology.

Most DMA measurements are made a single frequency and constant deformation (strain) amplitude while varying temperature. More informations can be provided with measurements in which the amplitude of the deformation is varied, and/or multiple frequencies are used [24]. All DMA clamp configurations feature a movable clamp and one or more stationary clamps, which are used to mount the sample. The movable part applies force and displaces the sample by stretching, bending, shearing or compressing it. The goal of DMA is to study the elastic and viscous responses of materials in the linear viscoelastic region (LVR), which means under low force conditions that do not destroy the structure. DMA is used to determine which conditions change the “original” viscoelastic behavior of the sample, and possibly lead to small irreversible deformation of the original structure. In fact, stress and strain of viscoelastic materials, including polymers, are a function of temperature, time, frequency, and the applied oscillation amplitude [25].

The relationship of stress and strain depends on the phase angle, which is a function of how much the polymer response lags behind the strain input. This relationship is used to derive trigonometric equations that produce three quantifiable properties that describe the sample response under the applied test conditions. They are the storage modulus, the loss modulus and the tangent of the angle δ . These properties are defined as:

$$\varepsilon = \varepsilon_0 \sin \omega t \quad (5)$$

$$\sigma = \sigma_0 \sin(\omega t + \delta) \quad (6)$$

$$\text{Storage Modulus} = E' = \frac{\sigma_0}{\varepsilon_0} \cos \delta \quad (7)$$

$$\text{Loss Modulus} = E'' = \frac{\sigma_0}{\varepsilon_0} \sin \delta \quad (8)$$

$$\tan \delta = \frac{E''}{E'} \quad (9)$$

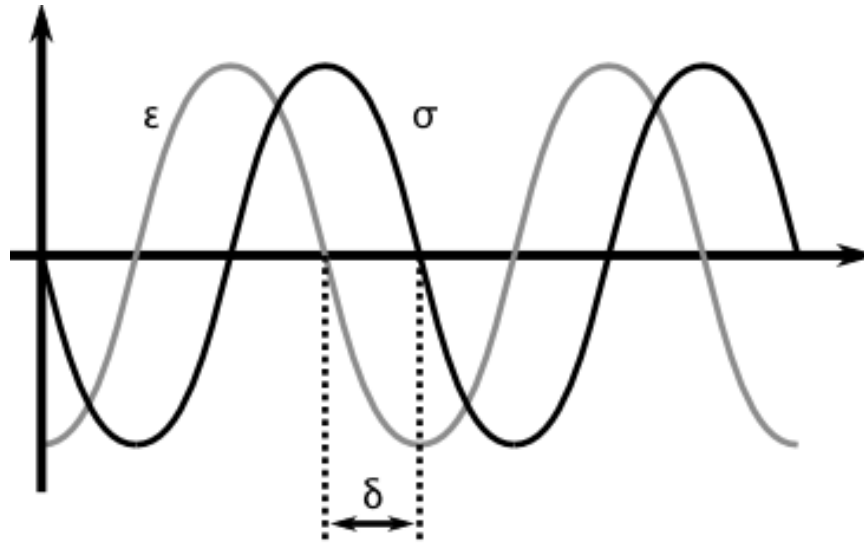


Figure 2.14 - Response of viscoelastic materials to a sinusoidal oscillation

The storage modulus corresponds to the mechanical energy stored by the material during a loading cycle. Consequently, it is related to the stiffness and the shape recovery of the polymer during loading. The loss modulus represents the damping behavior, which indicates the polymer's ability to disperse mechanical energy through internal molecular motions. The tangent of the angle δ is a sensitive indicator of the thermal/mechanical conditions that cause significant bond rotation or intermolecular friction and flow.

In this study, the DMA machine has been used to evaluate the variations of storage modulus, loss modulus and $\tan \delta$ in a temperature range from room temperature to 80 °C in order to compare these results with the ones obtained after the shear tests done with the MTS machine. Moreover, quasi-static tensile tests have been performed on the hot-melt adhesive sheets at room temperature and at 70 °C.

For all these tests, the thin film tension clamp shown in the figure 2.15 has been utilized after being properly calibrated. The baseline Bostik Thermelt 865 adhesive has been tested together with the modified HMAs with an addition of 30 % and 60 % in weight of metal microparticles in both small and big sizes.



Figure 2.15 - DMA Thin-film tension clamp [25]

Dynamic tests have been performed at constant frequency of 1 and 100 Hz with a temperature ramp of 0.5 °C/min from room temperature to 80 °C and a constant oscillation amplitude of 15 μm . Small pieces of adhesive sheets have been cut and clamped to the DMA machine with a torque screwdriver at a constant torque of 3 lb. in (0.339 Nm). The thickness and the width of the samples have been measured with a digital caliper while the length is evaluated by the

machine itself after clamping the specimen to it being known the distance between the fixed and the movable clamp.

The quasi-static tensile tests have been performed on specimens at room temperature and at a temperature of 70 °C. In the first case, the samples have been clamped to the DMA machine and pulled with a strain rate of 650 $\mu\text{m}/\text{min}$ until it failed. For what regards the high temperature tests, the specimens have been inserted in the DMA furnace and clamped at RT. A temperature ramp of 10 °C/min has brought the samples to a temperature of 70 °C. Then, the system has been left at constant temperature for 1 minute to obtain a more stable environment in the furnace. After this isothermal stop, the pulling phase started with a strain rate of 650 $\mu\text{m}/\text{min}$. Data have been collected after the experiments with the DMA post-processing software and graphs of the observed variables have been drawn and shown in the Chapter 5 of this work.

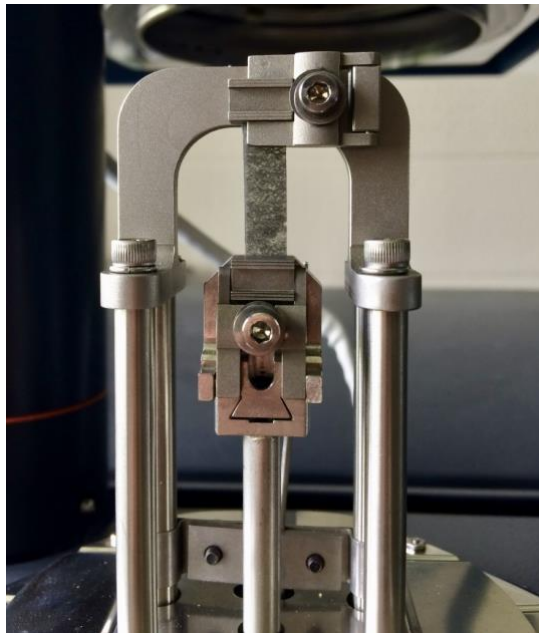


Figure 2.16 - DMA test setup – Adhesive sample with 60 % of small particles

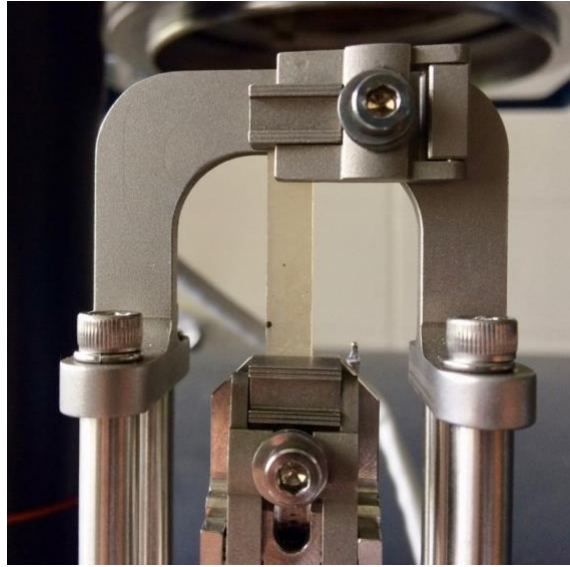


Figure 2.17 - DMA test setup - Pristine Hot-Melt adhesive

3 Preliminary tests

In this study, a preliminary phase has been required to evaluate the load transfer capacity of single lap joints of different adhesive-adherend combinations with the objective of finding the best combination in terms of LTC in order to select it for further analysis to be done with the selected adhesive in which metallic micro-particles have been embedded.

3.1 Materials screening

In this preliminary test phase, seven hot-melt thermoplastic adhesives and eight substrates have been tested. The objective is the evaluation of the adhesion performances of the different combinations in terms of load transfer capacity.

In the following table, the utilized adhesives are listed.

Table 3.1 - List of the Adhesives

Admer NE 827
Admer QF 500T
Admer QF 551T
Dow GR 204
Bostik TG 9446
Bostik Thermelt 865
Ellswort AP-122 H

The adhesives have been transformed from pellets to sheets in order to apply them on plaques of dimensions 4 x 2 x 0.1 inches (101.6 x 50.8 x 2.54 mm). The list of the selected substrates for this preliminary phase is presented in the Table 3.2.

Table 3.2 - List of the Substrates

High Density Polyethylene (Dow 12450 HDPE)
Nylon-6 (Akulon F136)
Polycarbonate (Sabic-Lexan 141)
Polycarbonate/ABS (Sabic Cycoloy 620S)
ABS (Ineos Lustran 433)
Zytel 70G33L NC010
Noryl GTX 910
Elastomeric Material

3.2 Methodology

The hot-melt adhesives that have been utilized in this test phase have been supplied in pellets. Admer NE827, QF500T, QF551T and Dow GR 204 are all characterized by a higher viscosity with respect to the other selected HMAs. Due to this fact, these four adhesives have required a pressure application at high temperature to obtain a sheet from their original pellets' configuration. To this purpose, the adhesives have been put into an oven for 10 minutes at constant temperature of 200 °C in a pan. Then, pressure has been applied by placing a second pan having the same dimensions of the first one onto the first pan. A load of 700 N has been applied over the system for 20 seconds.

The other three HMAs have shown a lower viscosity and they have been transformed into sheets only by means of heating provided with a heat gun without the need of any pressure application.

Each sheet of HMA has been cut into pieces with 0.5 in (1.27 mm) length and 2 in (5.08 mm) width to create the SLJs with a bonding area of 1 in² (6.45 mm²).

In this preliminary testing phase no surface treatment has been applied to the substrates.

The single lap joints have been prepared bringing the adhesive pieces to high temperature by means of a heat gun. The first half of joint has been pressed on the melted adhesive piece and then left cooling down to room temperature for 10 minutes. The heat gun has been utilized to heat again the HMA piece until reaching the melting temperature in order to apply on it the second half of the joint. A load of 20 N has been applied over the overlapped area of the joint for 15 minutes.

For each adhesive-adherend combination, three equal samples have been prepared and tested with a hydraulic tensile test machine produced by MTS in quasi-static shear tests. The setup of the experiments is the one that has been explained in the paragraph 2.1 of this thesis.

It is worth to highlight a particular procedure that has been required while testing the elastomeric material. In fact, due to the low resistance of the material to the pressure applied by the grippers of the MTS machine, metal spacers have been inserted on both sides of the halves of the joints to distribute better the pressure applied by the grippers. It has to be noted that the results obtained have been influenced by the strain of the substrates themselves and later by the one of the bonded areas.

Data have been recorded and the load vs. displacement curve has given information about the maximum load that each SLJ have sustained.

3.3 Preliminary results

In Tab. 3.1, the average values of the shear stresses are shown. The combinations for which the bonding has been unsuccessful have been highlighted with a red cell. Load vs. displacement curves and images of the broken specimens useful for a visual failure mode inspection are reported in the following pages for each tested hot-melt adhesive with the substrate that has shown the best performance with.

Table 3.3 - Preliminary results recap

	HDPE	Nylon 6	PC	PC/ABS	ABS	Elastomer	Zytel	Noryl
Admer 827	0.17	0.98	0.52	0.66			0.64	
Admer 500		0.32				0.32		
Admer 551	0.24					0.40		
Dow GR204	failed	0.25				0.25		
Bostik TG 9446	0.52	0.61	0.51	0.75	0.85	0.17	0.57	1.19
Bostik TG 865	0.23	1.13	1.28	0.94	1.88	0.15	0.84	1.45
Ellsworth AP-122H	0.56	0.42	0.37	0.48	0.58	0.09	0.24	0.89

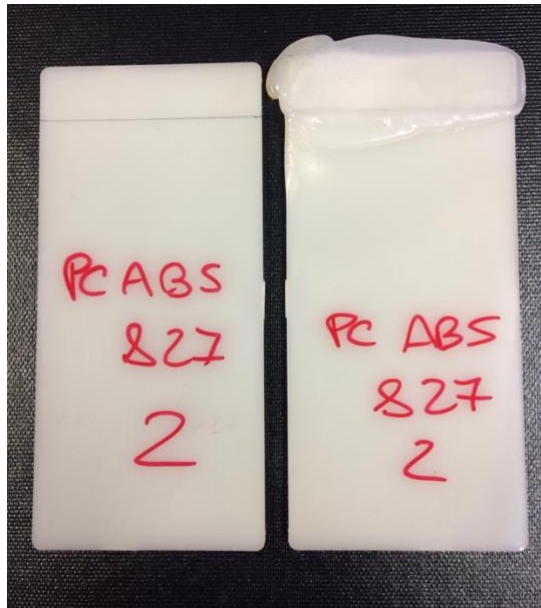


Figure 3.1 - Interfacial failure mode - PC/ABS substrate with Admer NE827

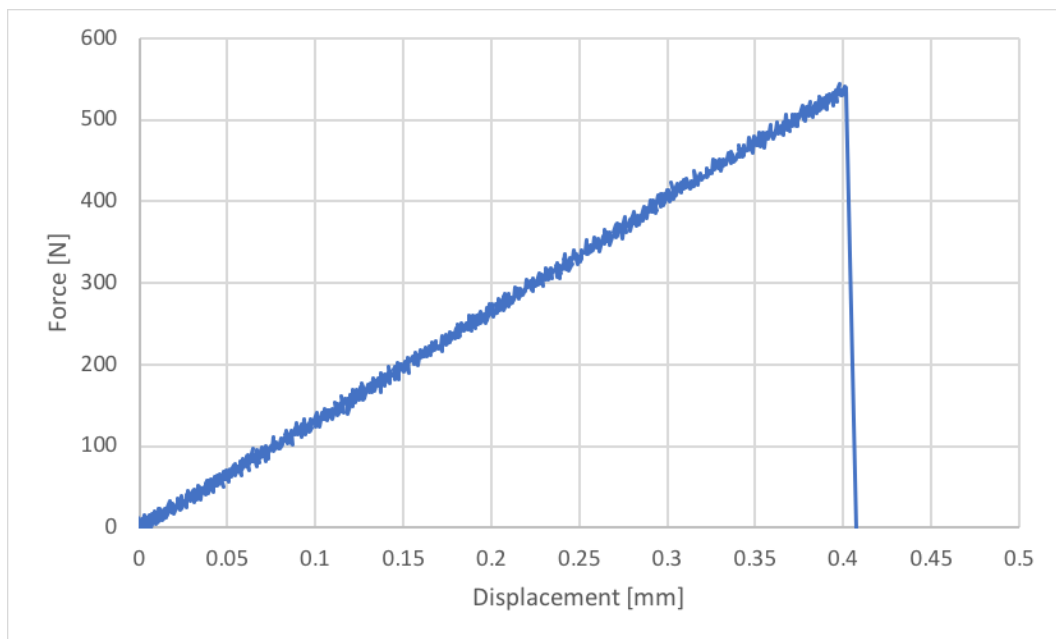


Figure 3.2 - Load vs. Displacement curve - PC/ABS substrate with Admer NE827



Figure 3.3 - Interfacial failure mode - Nylon 6 substrate with Admer QF500T

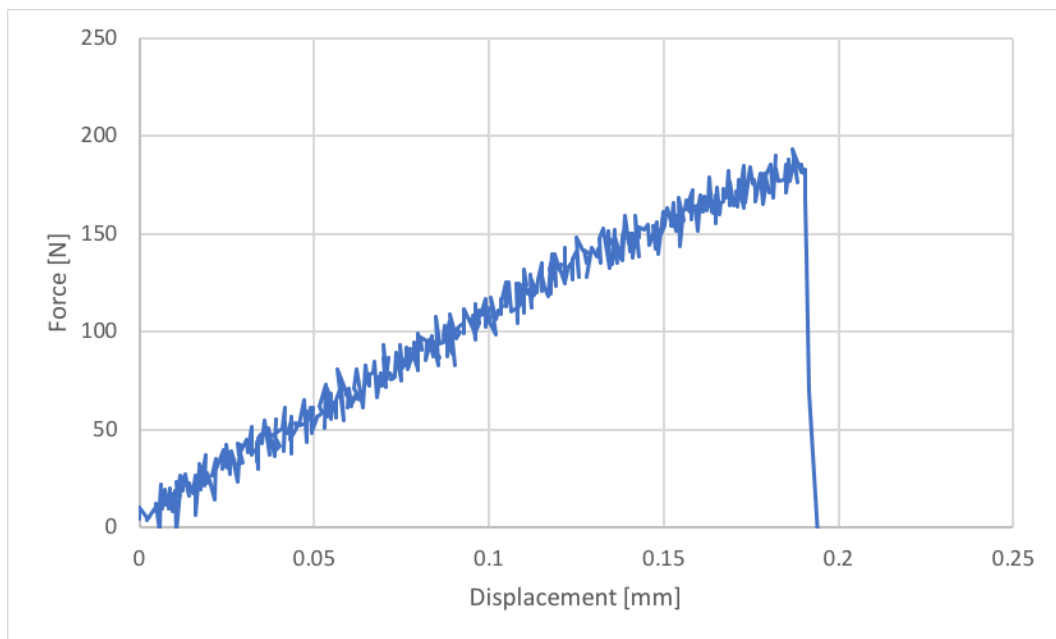


Figure 3.4 - Load vs. Displacement curve - Nylon 6 substrate with Admer QF500T



Figure 3.5 - Interfacial failure mode - HDPE substrate with Admer QF551T

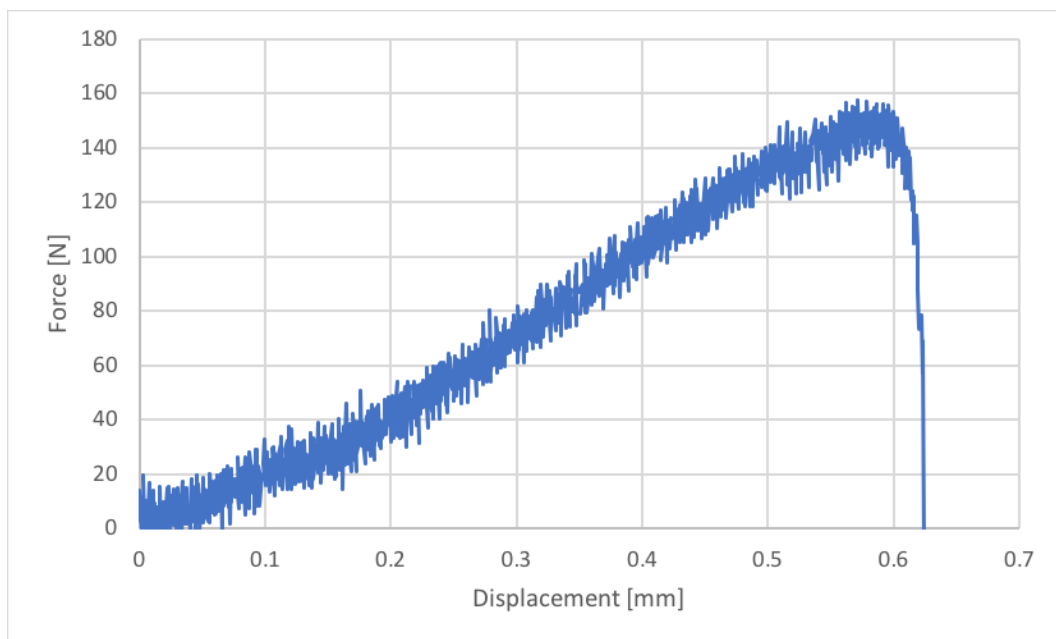


Figure 3.6 - Load vs. Displacement curve - HDPE substrate with Admer QF551T



Figure 3.7 - Interfacial failure mode - Nylon 6 substrate with Dow GR 204

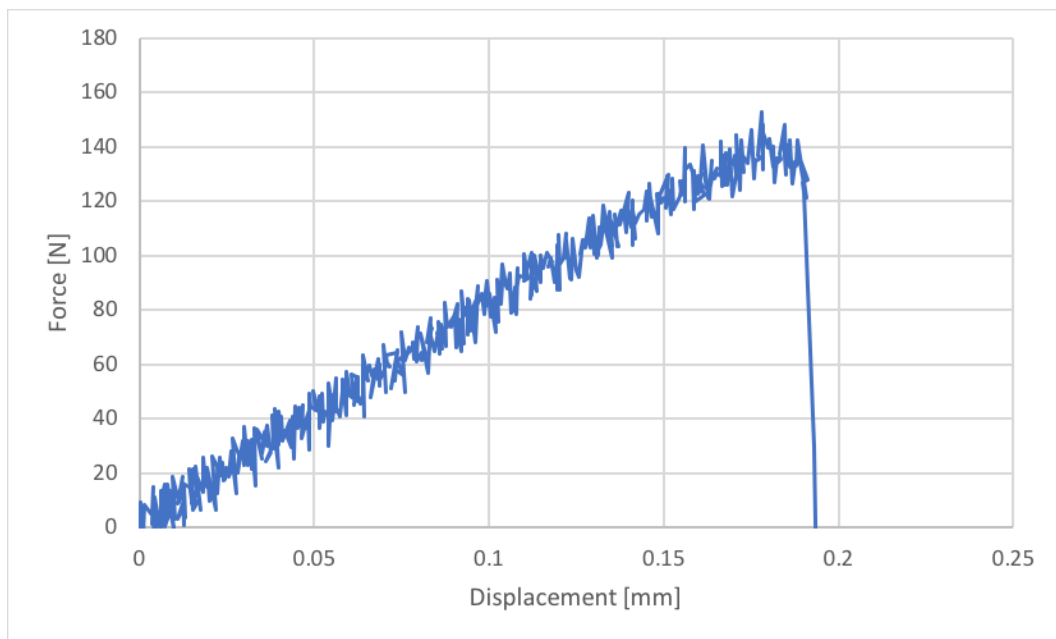


Figure 3.8 - Load vs. Displacement curve - Nylon 6 substrate with Dow GR 204

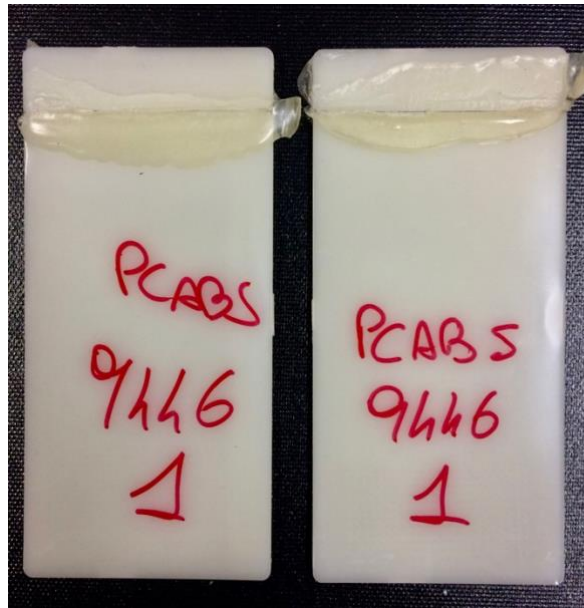


Figure 3.9 - Interfacial failure mode - PC/ABS substrate with Bostik TG 9446

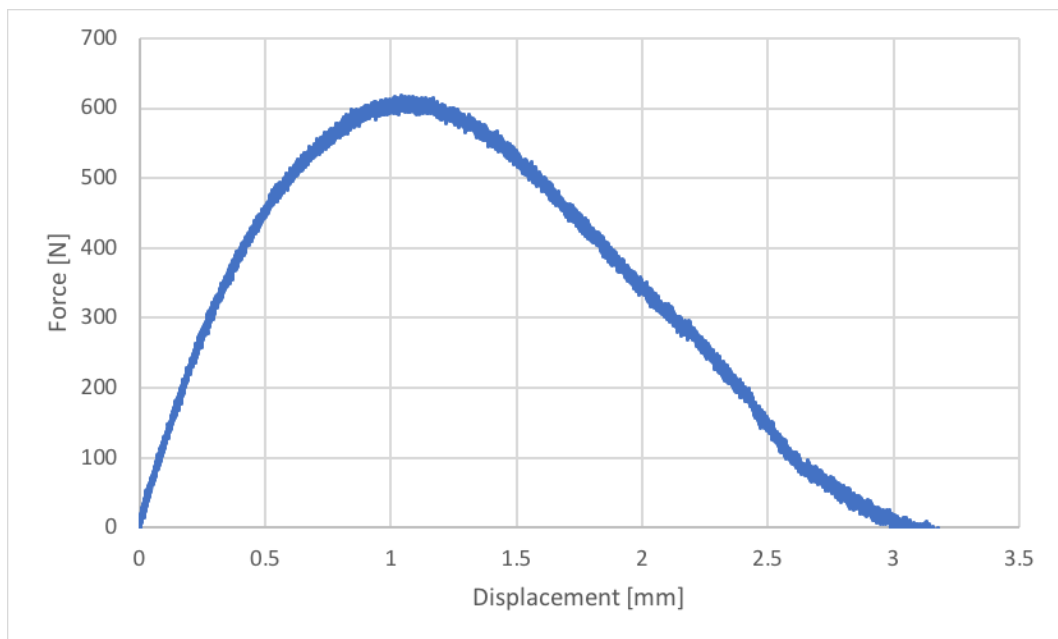


Figure 3.10 - Load vs. Displacement curve - PC/ABS substrate with Bostik TG 9446

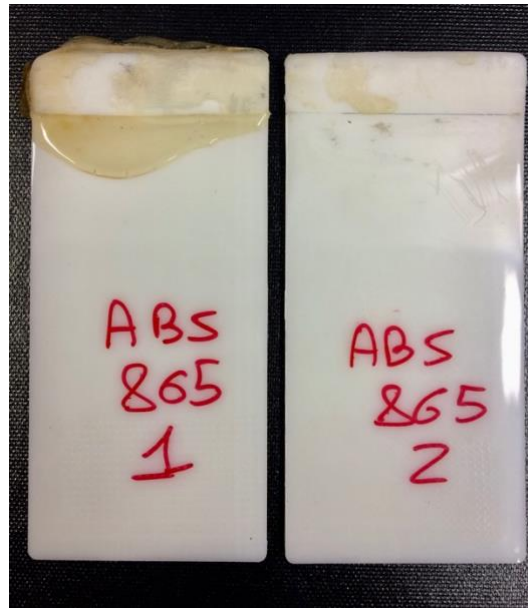


Figure 3.11 - Interfacial failure mode - ABS substrate with Bostik Thermelt 865

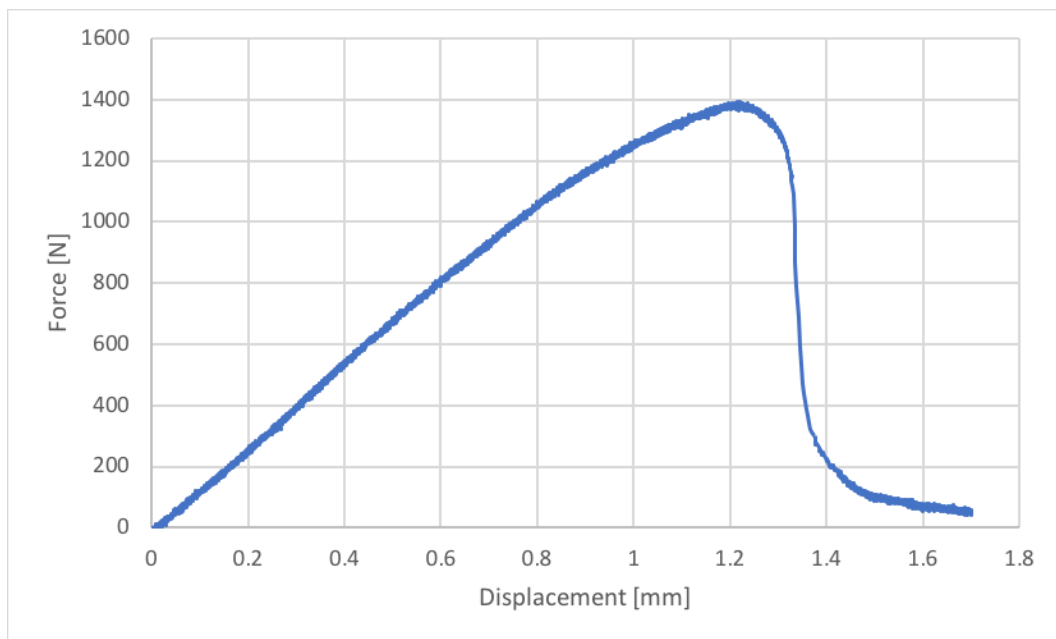


Figure 3.12 - Load vs. Displacement curve - ABS substrate with Bostik Thermelt 865



Figure 3.13 - Interfacial failure mode - ABS substrate with Ellsworth AP-122 H

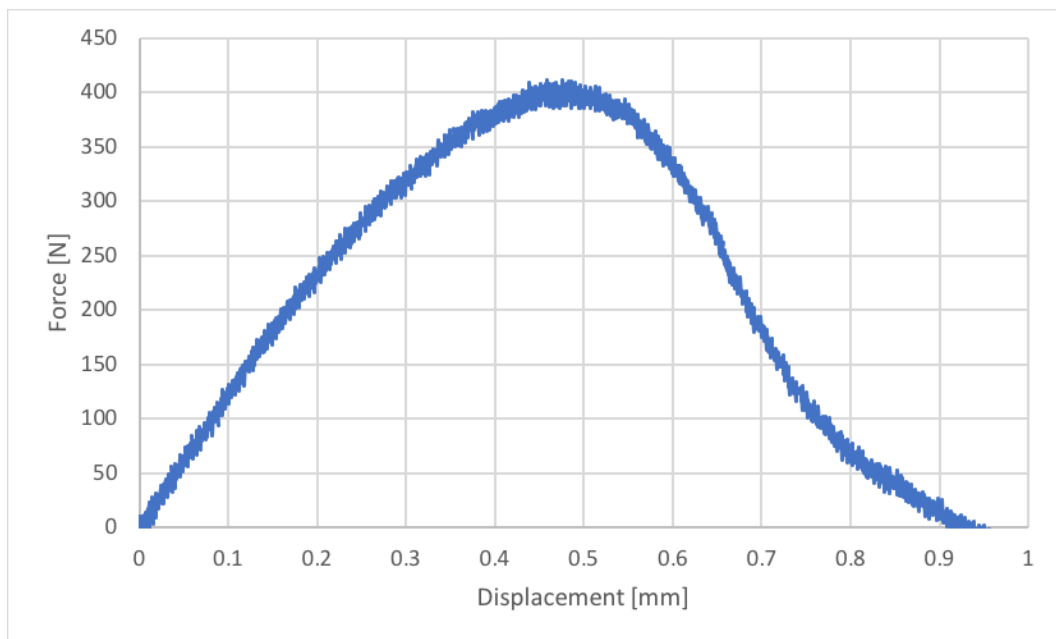


Figure 3.14 - Load vs. Displacement curve - ABS substrate with Ellsworth AP-122 H

After the execution of the quasi-static shear tests and the evaluation of the LTC of the single lap joints, the broken specimens have been observed to understand which failure mode occurred. It can be highlighted that interfacial failure mode has been observed in all the analyzed specimens thus meaning that the adhesion force between the adhesive and one of the two substrates have always been weaker than the intermolecular force inside the polymer regardless of the considered adhesive-adherend combination.

As it is shown in Table 3.1, the Bostik TG 9446, Bostik Thermelt 865 and the Ellsworth AP-122 H have been the only hot-melt adhesives for which the bonding process has been efficient with all the observed substrates. On the other hand, the Admer QF550T and QF551T and the Dow GR 204 have shown poor sticking capabilities with many of the utilized substrates and their correspondent results are under the average values of LTC obtained with the other substrates.

A particular mention can be done for the Admer NE827 that showed the highest performances among the group of the adhesives with higher viscosity and it could represent an interesting HMA to observe for further investigations due to the possibility of utilizing this polymer in injection molding processes thus increasing a lot the interest for industrial applications.

The objective of this first preliminary testing phase is to evaluate the adhesive-adherend combination that provides the highest average value in terms of load transfer capacity. It can be observed from the results in Table 3.1 that the Bostik Thermelt 865 has clearly provided the best results among the tested adhesives with many of the utilized substrates. In particular, the best result has been obtained with the Bostik Thermelt 865 as adhesive and the ABS as substrate.

The three repetitions of the test have shown an average result of 1.88 MPa for the lap shear strength with a standard deviation of 0.256 MPa.

Table 3.4 - Lap Shear Strength - ABS with Bostik Thermelt 865

	Shear Stress (MPa)
Test 1	2.16
Test 2	1.65
Test 3	1.84

Then, the Bostik TG 865 – ABS Lustran 433 combination has been selected for the following part of this thesis with the objective to analyze the differences in performance between the baseline adhesive and the modified one with the addition of susceptible iron particles in different weight percentages and sizes.

4 Manufacturing of test joints

In this section it is described the methodology that has been followed to manufacture the SLJs that have been tested for the second and main part of this work. After a brief description of the adopted adhesive and of the particles embedded in it, the steps that have led to the modification of the baseline adhesive and the to the manufacturing of the single lap joints is shown.

4.1 Material characteristics

Starting from the results obtained in the preliminary tests phase of this work, the Bostik Thermelt 865 has been selected for further investigations with the ABS Lustran 433 as substrate.

The Bostik Thermelt 865 adhesive is a pure copolymer polyamide hot melt resin, specifically designed for low molding pressure application. It is widely adopted for encapsulations of electronic parts in the automotive industry for external uses such as door locks and aerals. Adhesion is guaranteed on a wide range of substrates and offers cohesiveness up to -40 °C. In particular, it has been designed to obtain high adhesion on PVC and ABS substrates.

The main characteristics of the Bostik Thermelt 865 are reported in the table 4.1 [25].

Table 4.1 - Adhesive characteristics [26]

Minimum temperature for use [°C]	-55
Maximum temperature for use [°C]	120
Melting temperature [°C]	210
Softening point [°C]	158
Brookfield viscosity [Pa·s] @ 210 °C	3
Open time [s]	10
Tensile strength [MPa]	3
Elongation at break [%]	500
Glass transition temperature [°C]	55
Thermal conductivity [W/(m·K)] @ 23 °C	0.2



Figure 4.1 - Pristine HMA in pellets

In order to evaluate the performances of reversible thermoplastic adhesive, the polymer has been modified with the addition of iron microparticles. One of the variables that have been observed in this work is the size of the embedded particles. The dimensions of the iron particulate are presented in the following table in mesh scale and converted in millimeters.

Table 4.2 - Iron particles dimensions

Small Size Particles	-100 mesh	< 150 μm
Large Size Particles	-40/+325 mesh	44 μm < s < 420 μm



Figure 4.2 - Iron particles sizes - Smaller (left) and bigger (right)

The adherends that have been used for this study are made of ABS Lustran 433 compounded by Ineos Styrolution America LLC. The adopted plaques have been realized through an injection molding process and have length of 4 in (101.6 mm) and a cross section of 1 x 0.125 in² (25.4 x 3.125 mm²) according to the ASTM D3163 standard for adhesively bonded rigid plastic lap-shear joints in shear by tension loading. [18]

The main properties of the ABS Lustran 433 are summarized in the Tab. 4.3.

Table 4.3 - ABS Lustran 433 Technical data [27]

Specific gravity [/]	1.05
Linear mold shrinkage [cm/cm]	0.0040 – 0.0060
Melt flow @ Load 3.80 Kg and Temperature 230 °C [g/10 min]	3.6
Rockwell hardness	109
Izod notched impact strength @ 23 °C [ft·lb/in]	7
Tensile stress at yield @ 23 °C [psi]	6100
Tensile modulus [psi·10 ³]	370
Elongation at failure [%]	30
Drying temperature [°C]	175
Drying time [h]	4

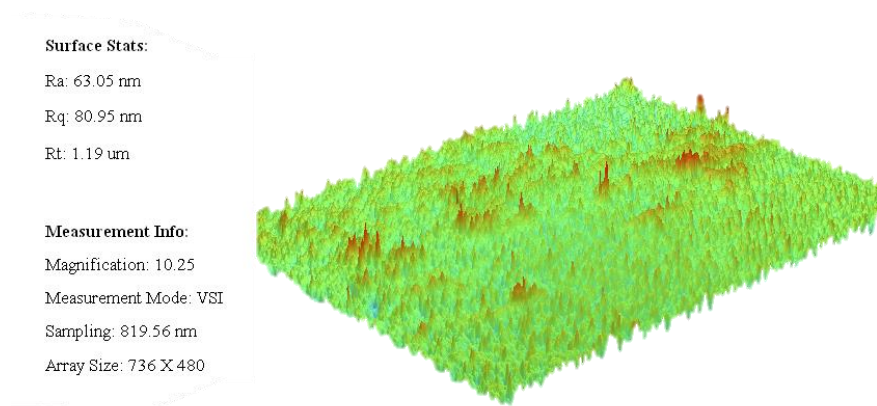


Figure 4.3 - Profilometer analysis - ABS substrate with no surface treatment

4.2 Preparation of the particle-enriched adhesives

The preparation of the adhesive to use for the following tests has been done in the Technology Center of “Emabond Solutions TM” in Norwood, NJ.



Figure 4.4 - Adhesive enrichment - Equipment

The low viscosity of the selected adhesive has not allowed the use of an automatic “Brabender” mixing machine due to problems of separation between particles and polymer that have ended up in a non-uniform composition of the modified adhesive. Therefore, the particles have been mixed in the adhesive manually.

In order to mix in a correct way the particles into the polymer matrix, the adhesive has been brought to melting temperature in an oven. Metal cans have been filled with 75 gr of baseline adhesive in pellets and let heat in the oven at constant temperature of 210 °C for 40 minutes.



Figure 4.5 - Oven

Particles have been added manually to obtain the required combinations in terms of weight percentages and mixed by means of a metal spoon exploiting the open time of the adhesive.

$$mass\ of\ particles\ [gr] = \frac{75\ gr * particles\ weight\ \%}{100 - particles\ weight\ \%}$$

Then, the modified adhesive has been left cooling down to room temperature for one hour before pressing it to obtain a constant thickness sheet.

For the pressing phase, it has been utilized a metal mold with dimensions:

- 4 inches (101,6 mm) of length
- 4 inches (101,6 mm) of width
- 0.035 inches (0,9 mm) of thickness

Being known the volume of the adhesive to be pressed in the mold, the required amount of adhesive has been calculated estimating the average density of the compound imposing the density of the particles to 7.8 g/cm³ and the one of the adhesives to 1 g/cm³.

The result is summarized in the following table. For each press, 1 extra gr has been added to avoid voids in the pressed sheet.

Table 4.4 - Mass of compound required for pressing phase

Particle Weight %	Density (g/cc)	Density (lbs/cu.in)	Mass (lbs)	Mass (g)
5	1,05	0,038	0,02128	9,65243776
10	1,1	0,040	0,0224	10,1604608
20	1,21	0,044	0,02464	11,17650688
30	1,35	0,049	0,02744	12,44656448
40	1,54	0,055	0,0308	13,9706336
50	1,77	0,064	0,03584	16,25673728
60	2,1	0,076	0,04256	19,30487552
70	2,57	0,093	0,05208	23,62307136

The mold has been placed between two metal sheets with two Teflon sheets between them. The press machine has been brought to a temperature of 200 °C on each side.



Figure 4.6 - Pressing machine

The pressing phase has been divided in the following four phases:

- 5 minutes of heating with no pressure application
- 5 minutes of heating with 200 N of load applied
- 5 minutes of heating with 450 N of load applied
- 5 minutes of cooling with 450 N of load applied

The same procedure has been followed for the preparation of all the required combinations of modified adhesive varying size and weight percentages of the iron. In order to study the effects of the addition of the particles into the polymer matrix with respect to the pristine adhesive, an equal sheet of baseline Bostik Thermelt 865 has been realized with the same procedure.

Samples of pressed sheets are shown in the following figure. The baseline (a) and two configurations with the bigger particles, namely 30 % (b) and 60 % (c), are presented.

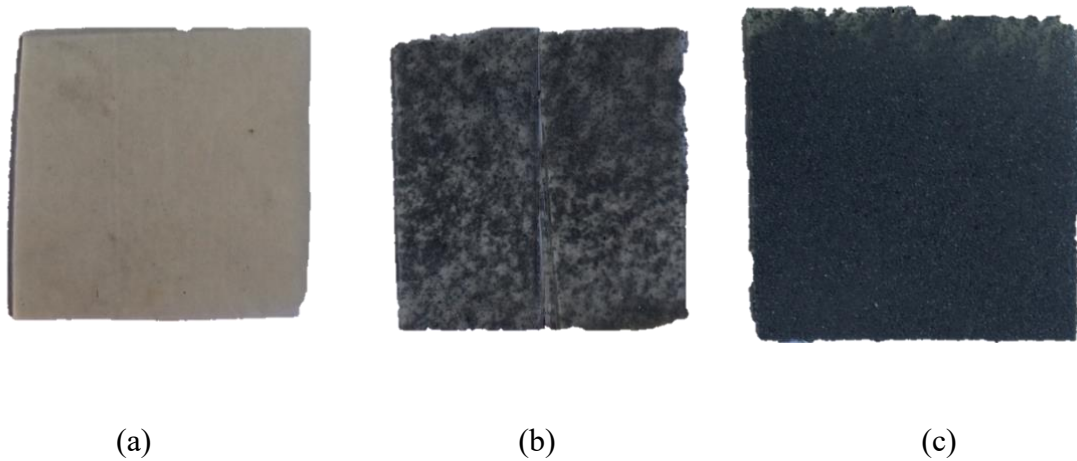


Figure 4.7 - Adhesive sheets - Baseline (a), 30 % (b) and 60 % (c) big particles

Microscope scanning of four modified adhesive sheets are provided. An optical microscope has been used with a magnification of 50x. The difference between the sheets in two different weight percentages (20 % and 70 %) of added iron particles in two sizes is shown.

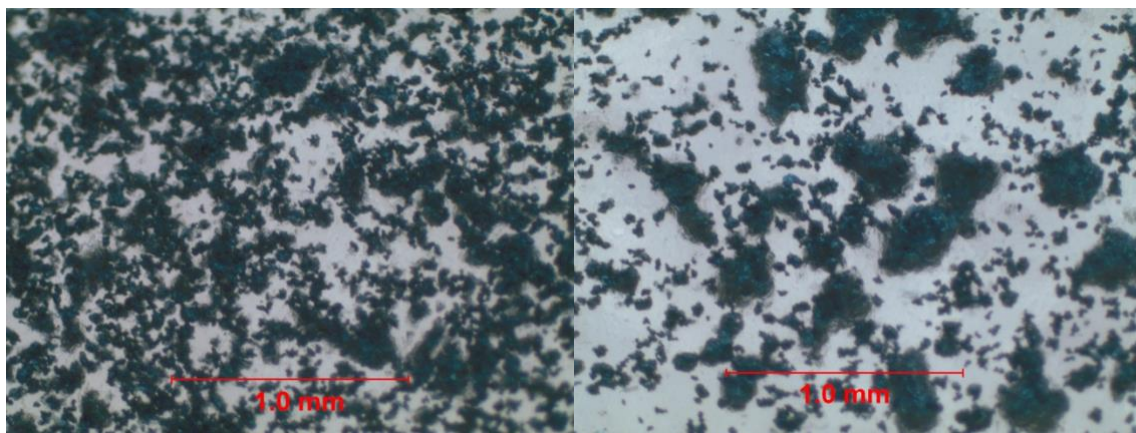


Figure 4.8 - Optical microscope scanning, 50x magnification - HMAs with 20 % of small (left) and big (right) iron particles

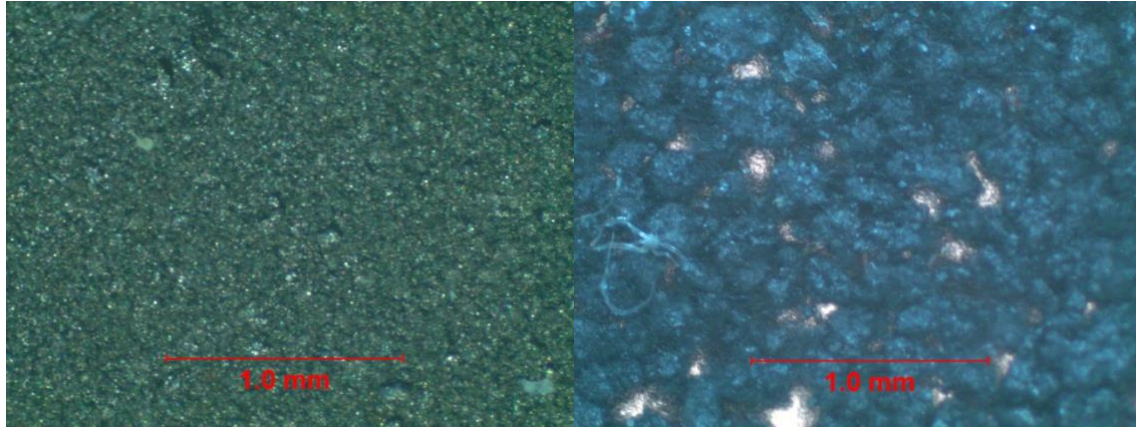


Figure 4.9 - Optical microscope scanning, 50x magnification - HMAs with 70 % of small (left) and big (right) iron particles

4.3 Assembling process

The selected ABS substrates have been treated with acetone to avoid the presence of unwanted materials on the bonding area and to reduce the unevenness obtained after the injection molding process. The surface treatment has been made by means of a cloth moved longitudinally on the adherend.

The sheets of modified hot-melt adhesive have been cut in pieces of 1 in (25.4 mm) length and ½ inch (12.7 mm) width to create single lap joints according to the ASTM D3163 standards.

The bonding process has been performed exploiting the iron particles thermal sensitivity to electromagnetic field. A custom designed machine has been adopted to create the single lap joints. The machine generates an electromagnetic field with a fixed frequency of 13.56 MHz and its emitted power can be set up to 3.5 KW. In order to obtain repeatable and controllable processes with all the considered combinations, all the joints have been assembled with a power of 500 W. The correspondent voltage is in the range of (2350 : 2450) V.

The capacitors of the machine have been tuned to have a null value of the reflected power in order to have all the actual power emitted in the correct way.

The coil that has been used for the bonding of the joints is the one presented in the Fig. 4.4. It is made of a single turn of copper. The overall length is 600 mm and the cross section is squared with an area of $1/16 \text{ in}^2$ (40.32 mm^2). The coil is connected by means of bolted joints to the machine and with plastic hoses to the refrigerating system that lowers the temperature at the end of the bonding process. For the adopted coil, the controller parameters that gave the best performances in terms of ratio between emitted and reflected power have been defined: the tune has been set to 14 % and the load to 44 %. This setup has allowed a use of the bonding machine with less than 0.5 % of reflected power.

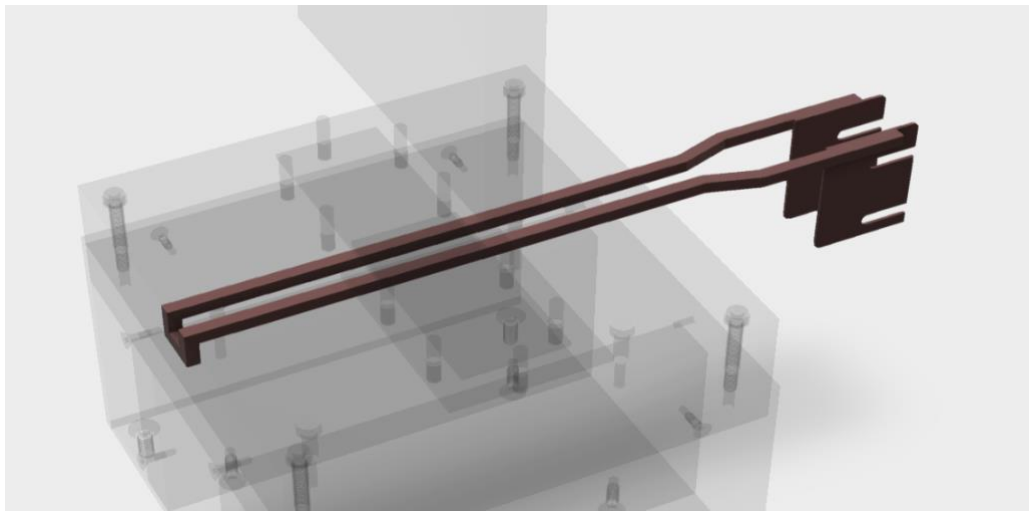


Figure 4.10 - CAD Scheme of the coil

The coil has been inserted in a custom-built fixture made of Teflon in which holes have been drilled to insert metal pins that helped the positioning of the substrates. Thermoresistant tape has been placed in the area of the fixture in which the samples were located to avoid damaging

of the coil due to eventual material squeezing during the process. A spacer of Teflon with a thickness of 0.15 in (3.8 mm) has been placed on the fixture to obtain a better alignment of the two halves of the joint when bonded together.

The overall scheme of the bonding machine is presented in the figure 4.11.

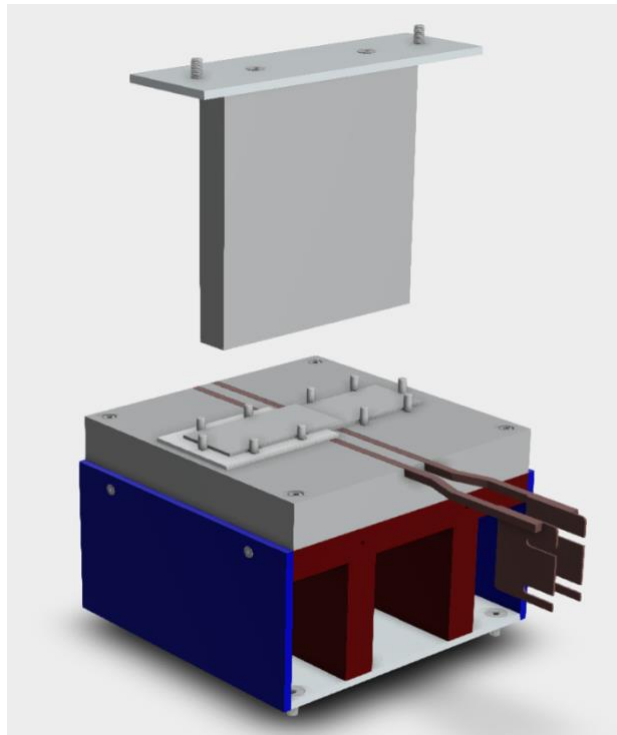


Figure 4.11 - CAD Scheme of the bonding machine

The bonding process parameters have been evaluated after preliminary tests made with only one of the two halves of the joint located close to the coil with a piece of adhesives laying on it.

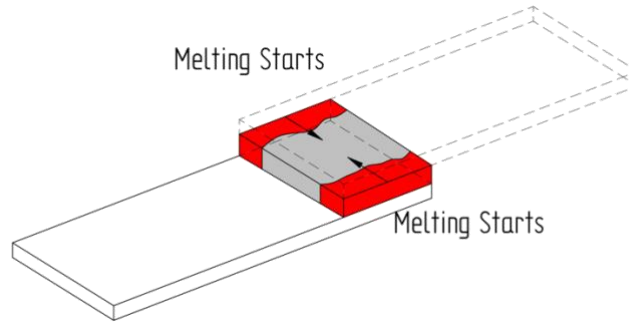


Figure 4.12 - Path of melting process

The sample has been placed with the bonding area inserted between the two branches of the coil to exploit best the electromagnetic field. It has been observed that the melting process started from the edges of the adhesive piece going through the central part as explained in Fig. 4.12. In order to define the time required to obtain a complete melting of the adhesive sheet, a LCR thermometer that changes color at 400 °F (204 °C) has been used.

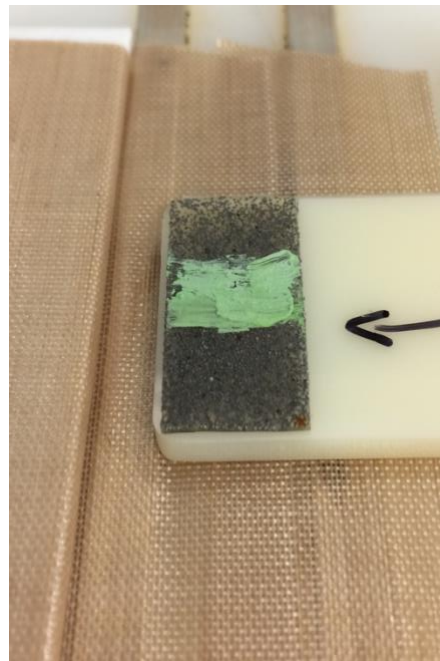


Figure 4.13 - Bonding process - Time evaluation with LCR Thermometer

The actual bonding time that has been selected is the one observed during the tests with the LCR thermometer with an addition of 5 % in time to consider also the different heat transfer coefficient of the system when also the second half of the joint is located in position to bond the samples.

The resulting bonding time required for each combination of modified adhesive are shown in the Fig. 4.14. It can be observed that the time needed for the complete melting of the adhesive decreases with a trend that may be approximated to a 2nd order polynomial. Moreover, it can be noticed that the bonding time for the modified HMAs with the bigger iron particles is lower than the time required by the correspondent combination with the smaller particles. This result is obtained due to the higher value of heat transfer coefficient of the bigger micro-iron particles that are excited by the high-frequency electromagnetic field.

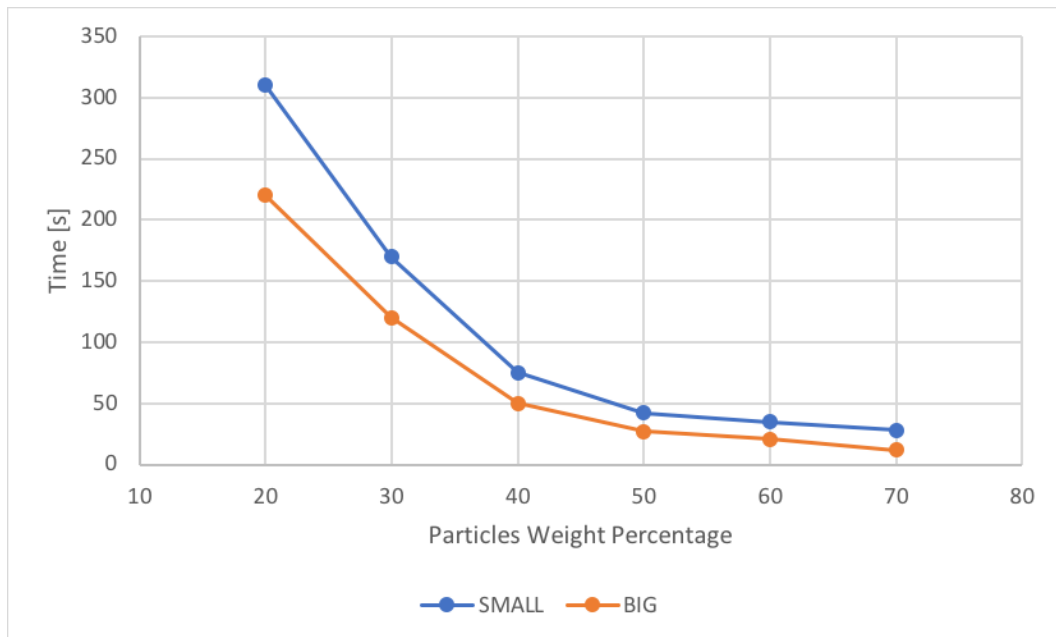


Figure 4.14 - Time to complete bonding process

After the heating phase under the action of the electromagnetic field, a load of 100 N has been applied to the bonding area for 10 seconds to enhance the joining phase. Later, the samples have been left cool down for 3 minutes with a load application of 30 N before being stored.

5 Test data and discussions of results

In this section, test data and observations are presented and discussed for the quasi-static shear tests, for the debonding experiments and for the test performed with the Dynamic Mechanical Analyzer.

5.1 Quasi-static tensile-shear tests of Single Lap Joints

The quasi-static shear tests have been performed with the MTS hydraulic tensile machine on the baseline HMA and on the modified adhesives with the addition of iron micro-particles in the polymer matrix in two different sizes and in a weight percentage of 20 %, 30 %, 40 %, 50 %, 60 % and 70 % of the total mass of the compound.

In the Fig. 5.1, it is shown the trend of the average lap shear strength expressed in MPa that has been measured on the samples tested at room temperature.

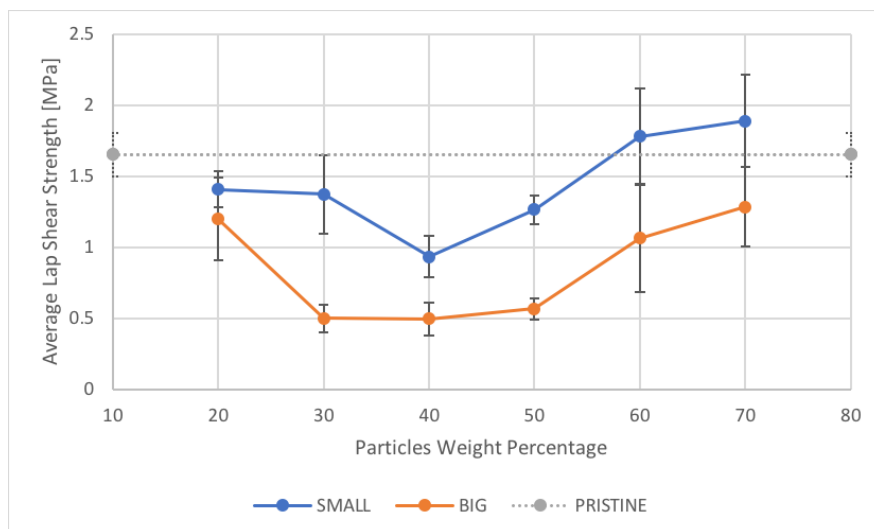


Figure 5.1 - Effect of particulate size - Room Temperature Baseline

The average stress obtained with the tests on the pristine adhesive is 1.65 MPa and it has been as reference value in the previous graph. The correspondent standard deviation is 0.16 MPa. For what regards the modified HMAs, the increase of the weight percentage of the particles has given for both the considered particulate sizes a reduction in the performance of the bond with respect to the pristine one. The obtained data clearly highlight a difference in performances between the two particulate sizes. Having fixed the weight percentage of metal particles, the lap shear strength of the specimens with the smaller size of the particulate has been higher than the one obtained with the bigger particles in a range that goes from the 15 % to the 64 %.

It is worth to notify that the trend of the results shows decreasing values of shear stress in the first half of the observed range of weight percentages reaching a minimum value of 0.49 MPa for the adhesive with 40 % of bigger iron micro-particles mixed to the pristine adhesive. These results agree with the ones previously obtained by Banea et al. [8] that have identified the reason of this behavior in the changes of the adhesive structure and of the bond-line characteristics due to the presence of the particles in the matrix.

The trend is reversed increasing the weight percentage of iron in the matrix to values that are bigger than 50 %. In particular, the lap shear strength that has been measured for the samples with 60 % or 70 % mass of the smaller iron particles is equal to 1.78 and 1.89 MPa respectively thus meaning a higher value than the reference one of the pristine adhesive. This result may be explained considering the fact that a so high mass ratio between metal particulate and polymer tends to create mechanical friction between the particles that cannot be neglected in the overall amount of shear strength. Moreover, micro-welding phenomena among the iron particles may occur increasing the strength of the bond in localized regions of the overlap area.

In the Figure 5.2 and 5.3, the load vs. displacement curves of two of the performed tests are shown. It can be observed that the curve referred to the specimen with the 20 % of added particles is similar to the one of the pristine adhesive (Fig. 3.12), while it differs in the case of

the sample with the enrichment of 70 % of metal particles. This phenomenon may explain the high strength values of the SLJs with a high percentage of mixed iron in which it is the iron the main responsible of the LTC of the sample. Mechanical friction and particles' welding overcome the strength of the adhesive itself and keep the two halves of the SLJs bonded up to a more abrupt failure without any type of residual stress as it was observed in the case of pristine and modified HMAs with low amount of particles.

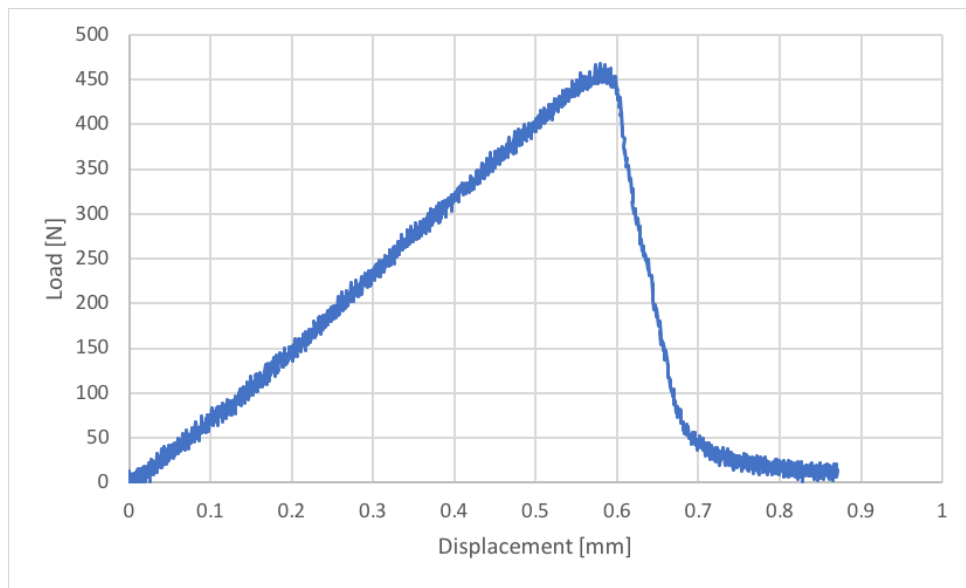


Figure 5.2 - Load vs. Displacement curve - HMA with 20 % of smaller iron particles

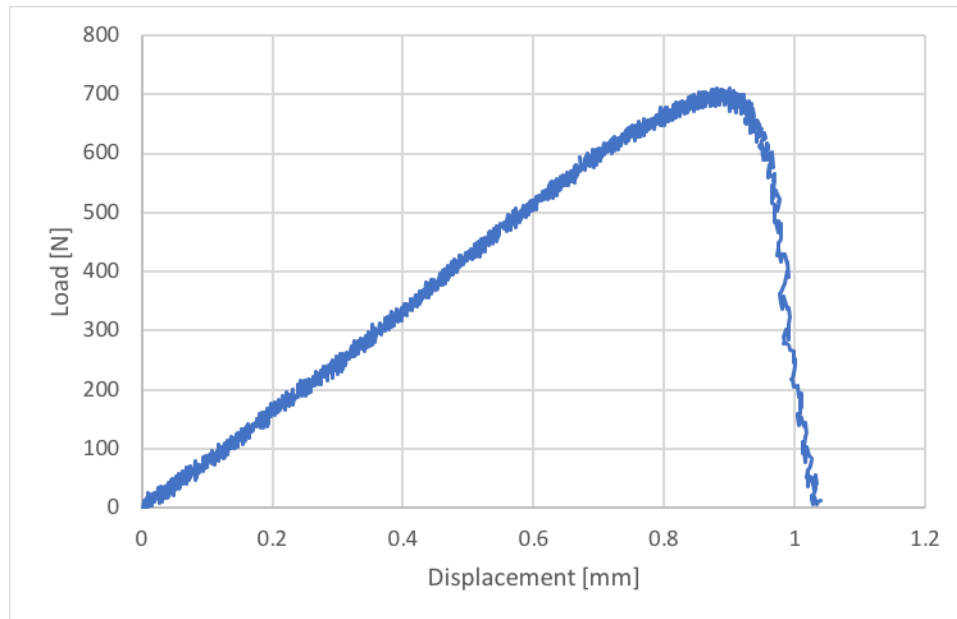


Figure 5.3 - Load vs. Displacement curve - HMA with 70 % of smaller iron particles

The failure mode of the samples has been observed by a visual inspection. All the specimens that have been tested have shown an interfacial failure mode, regardless the particulate size or the level of enrichment.

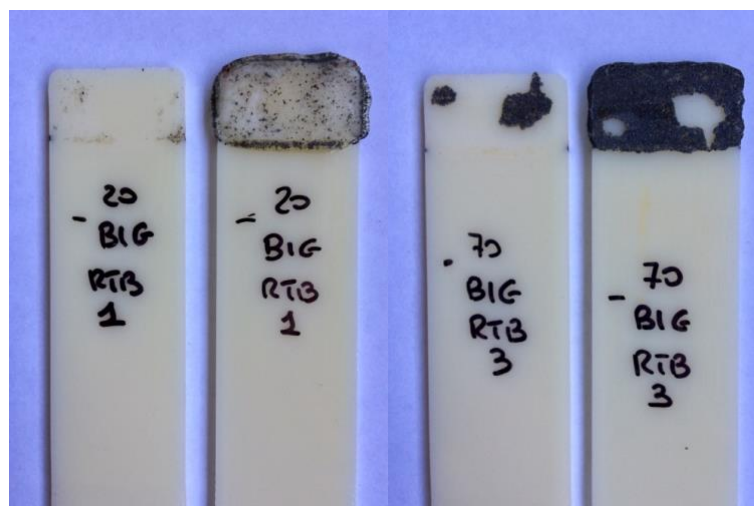


Figure 5.4 - Interfacial failure mode - Room Temperature with 20 % (left) and 70 % (right) of “big” iron particles

The specimens have also been tested after being subjected to a controlled temperature-humidity cycle in a Thermotron environmental chamber. In the Fig. 5.5, the results of the quasi-static shear tests on these samples are presented.

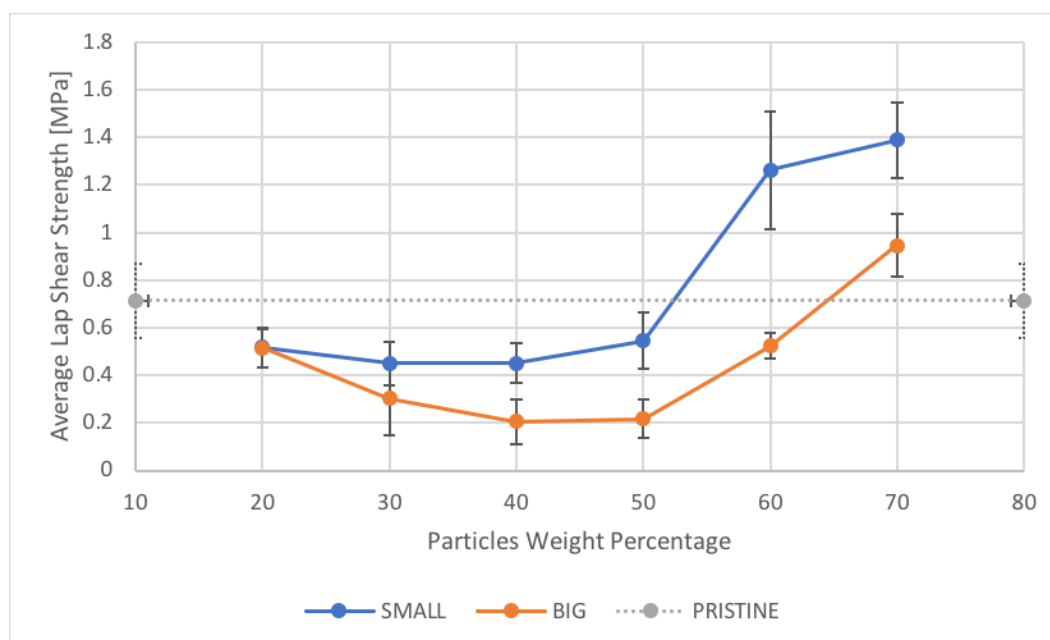


Figure 5.5 - Effect of particulate size - Room Temperature after env. cycling

In this case, the obtained reference value of the pristine hot-melt adhesives is equal to 0.71 MPa with a standard deviation of 0.16 MPa. As it has been observed for the tests on the baseline specimens, also the results on the environmentally cycled samples show higher performances in terms of average lap shear strength for the SLJs with the HMAs in which the smaller iron particles have been added.

The trend of performances is similar to the one observed for the baseline case study. For both particulate sizes, the strength is decreasing up to an iron weight percentage of 40 % and then starts to increase to values that are bigger than the ones obtained with the pristine adhesive and reach a peak value of 1.39 MPa observed with the modified HMA with the 70 % of weight of the smaller iron micro-particles.

It is worth to highlight the overall reduction in the performances of these samples with respect to the SLJs that have not been subjected to the temperature-humidity environmental cycle. The presence of the moisture in the polymer is the main cause of this drop of lap shear strength. In fact, moisture is absorbed into the HMA chemical structure and tends to decrease the strength of molecular bonds. In the Fig. 5.6 and Fig. 5.7, it is provided a comparison between the results of the shear tests performed on baseline joints and on the environmentally cycled ones.

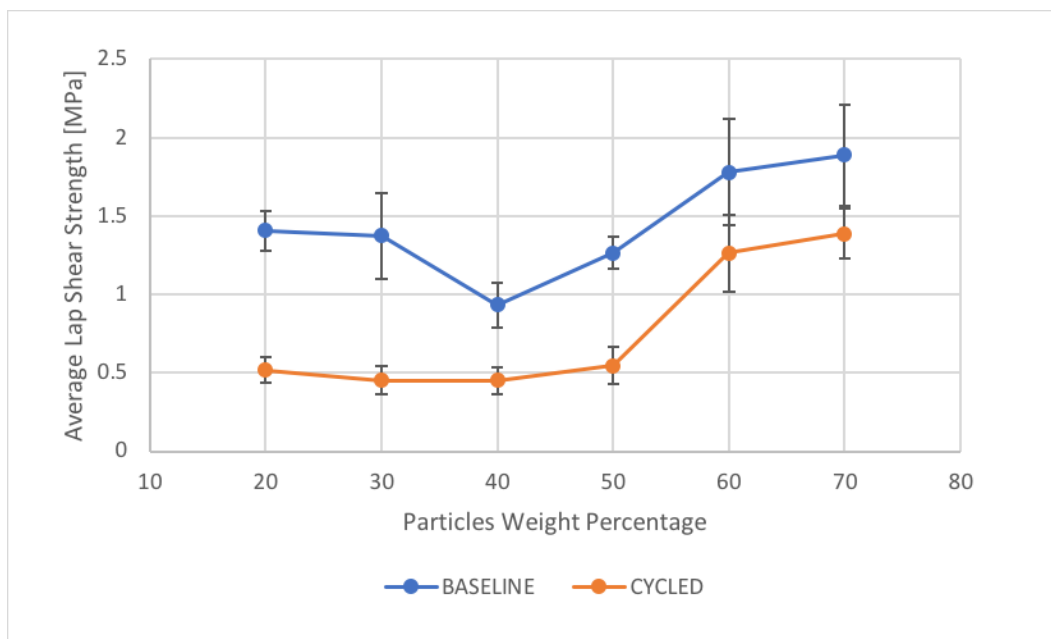


Figure 5.6 - Effect of environmental cycle - Room Temperature - Small particles

It can be highlighted that the reduction in terms of average lap shear strength has bigger values for the samples with a smaller iron weight percentage. The performance drop is kept in a range that goes from 26 % to 61 %.

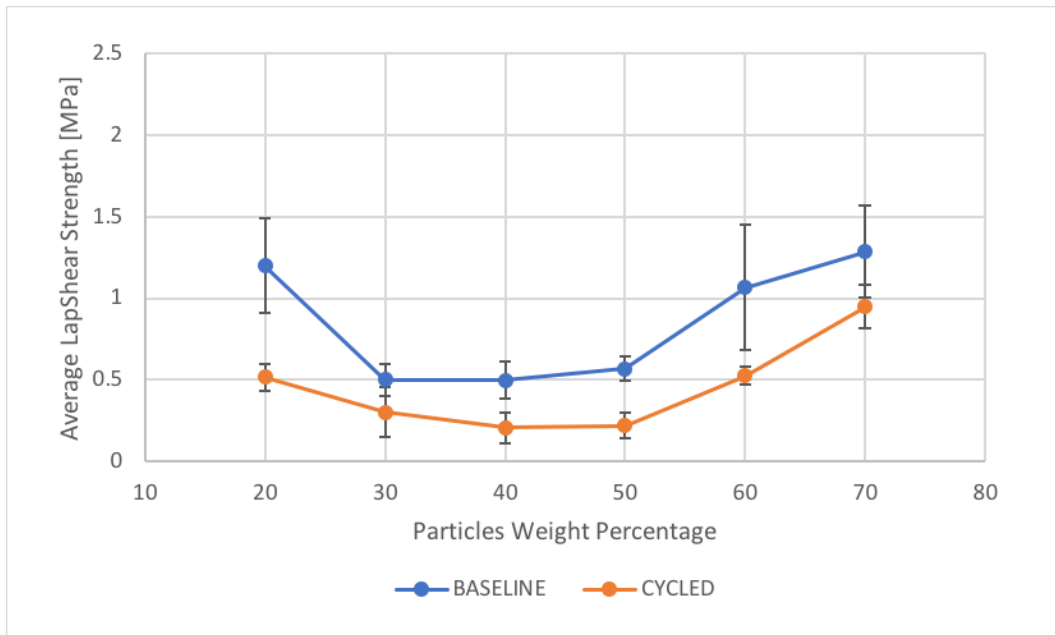


Figure 5.7 - Effect of environmental cycle - Room Temperature - Big particles

Also in the case of the specimens exposed to environmental cycling, the observed failure mode has been on the edge between the modified adhesive and one of the two ABS plaques.

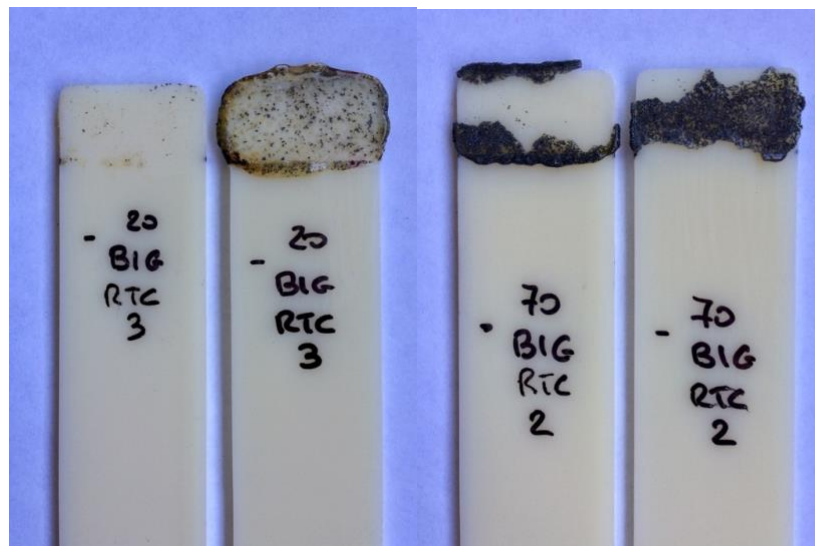


Figure 5.8 - Interfacial failure mode - Room Temperature after environmental cycle with 20 % (left) and 70 % (right) of “big” iron particles

The quasi-static shear tests have also been performed at a temperature of 70 °C on both baseline and environmentally cycled. The MTS hydraulic testing machine has been equipped with its environmental chamber to test the specimens at high temperature and the test setup has been based on the output of the FEM simulation model that has been presented in the section 4.2.

The experiments have shown a remarkable drop in the performance of the adhesive both in pristine and modified configurations. The load transfer capacity of the single-lap joints has dropped to values always smaller than 100 N thus corresponding to average values of lap-shear strength in the range between 0.12 and 0.18 MPa for the baseline specimens and between 0.09 and 0.12 MPa for the cycled ones. The reference value of the pristine adhesive has been set to 0.32 MPa for the baseline samples and to 0.23 MPa for the environmentally cycled ones with a standard deviation of 0.05 and 0.02 MPa, respectively.

It can be noticed that the addition of iron micro-particles in the compound has reduced the strength of the joint to values around 50 % with respect to the pristine adhesive and that the influence of the weight percentage is negligible in this case study. In the Fig. 5.9 and 5.10 the average lap shear strength for the tests on baseline and after-cycled samples is shown. It is worth to observe that also the differences in performance of the joints are very small between tests with the two different particulate sizes.

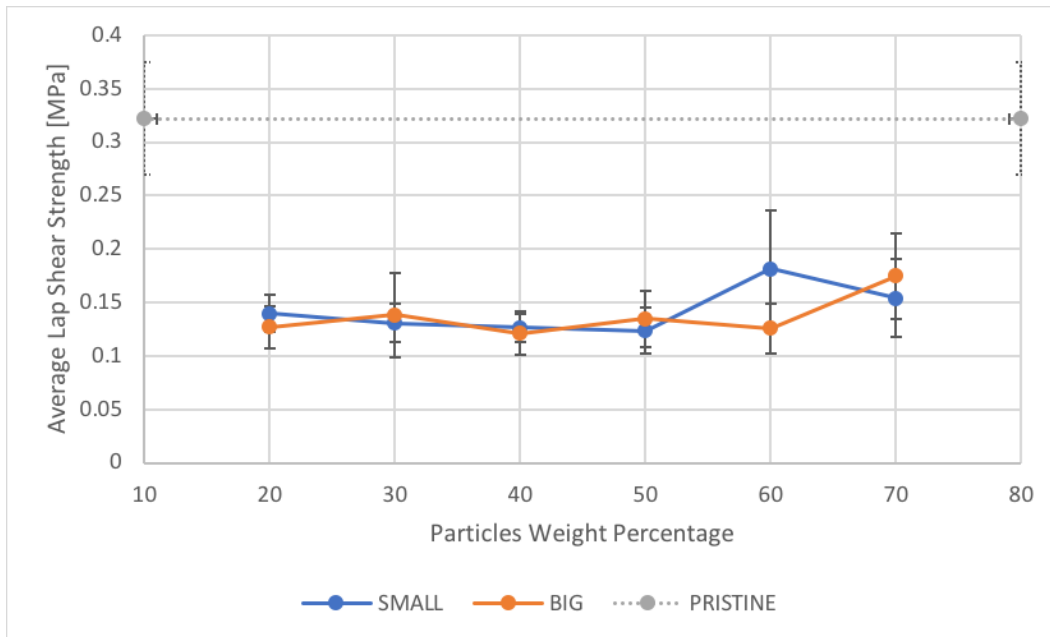


Figure 5.9 - Effect of particulate size - High Temperature Baseline

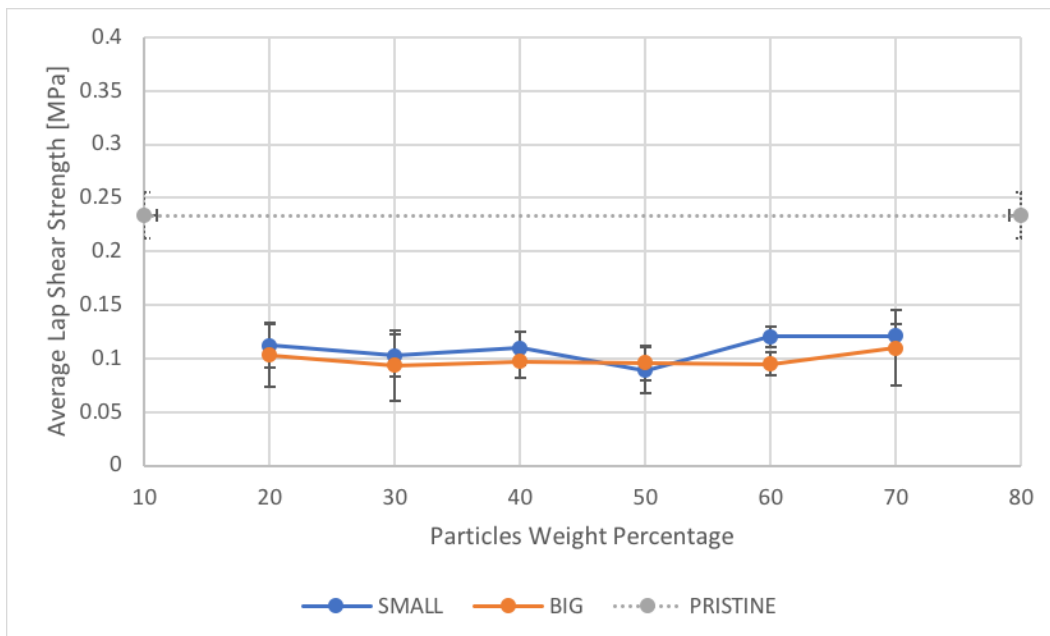


Figure 5.10 - Effect of particulate size - High Temperature after env. cycling

The controlled temperature-humidity environmental cycle has had a worsening effect on the joint. The presence of moisture also in this case reduces the lap shear strength of values that stays in a range between 13 % and 34 % as is shown in Fig. 5.11 and 5.12.

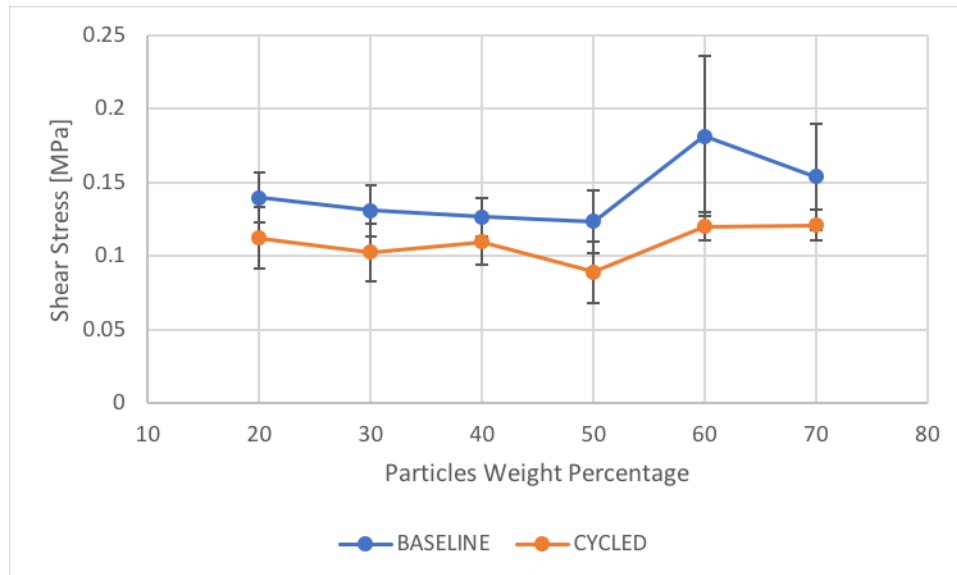


Figure 5.11 - Effect of environmental cycle - High Temperature - Small particles

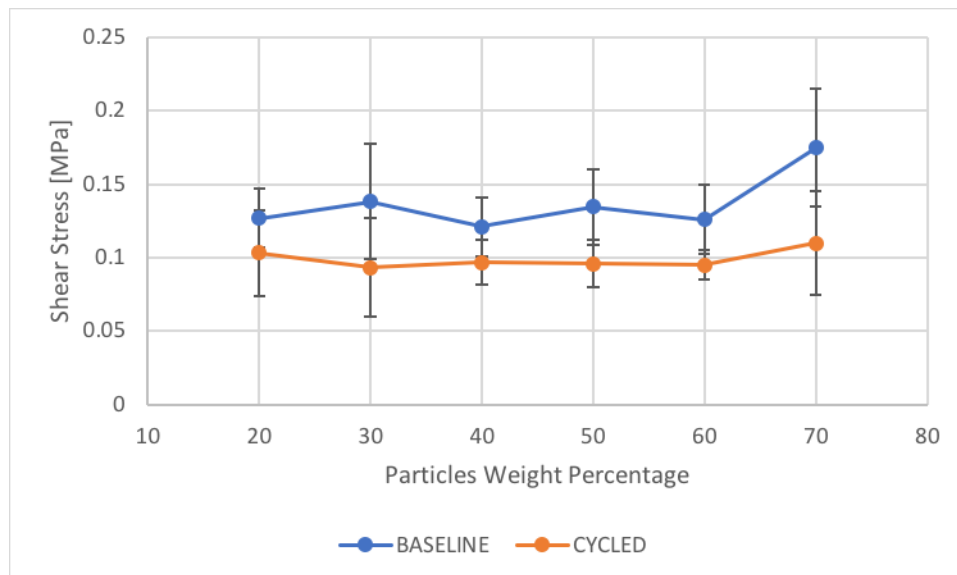


Figure 5.12 - Effect of environmental cycle - High Temperature - Big particles

The tests at high temperature have shown the very poor performances of the selected hot-melt adhesive in these conditions. This result represents an important limit to the application of this HMA in environment that can be exposed to relatively high temperature such as a usage in the automotive field. In fact, the most important factor that has to be considered in the modification of the performances in terms of strength is represented by the test temperature. The reduction of the lap-shear strength that is obtained by testing the specimens at 70 °C instead of room temperature is much more relevant than the one obtained by modifying the particulate sizes and the weight percentage of the added particles or by subjecting the samples to an environmental cycle.

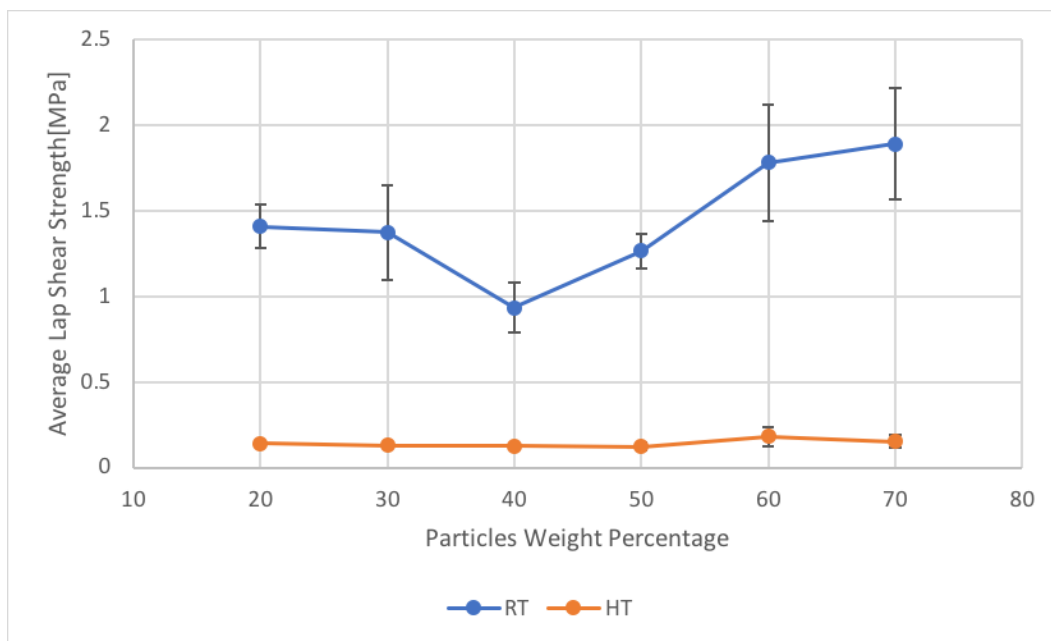


Figure 5.13 - Effect of testing temperature - Baseline - Small particles

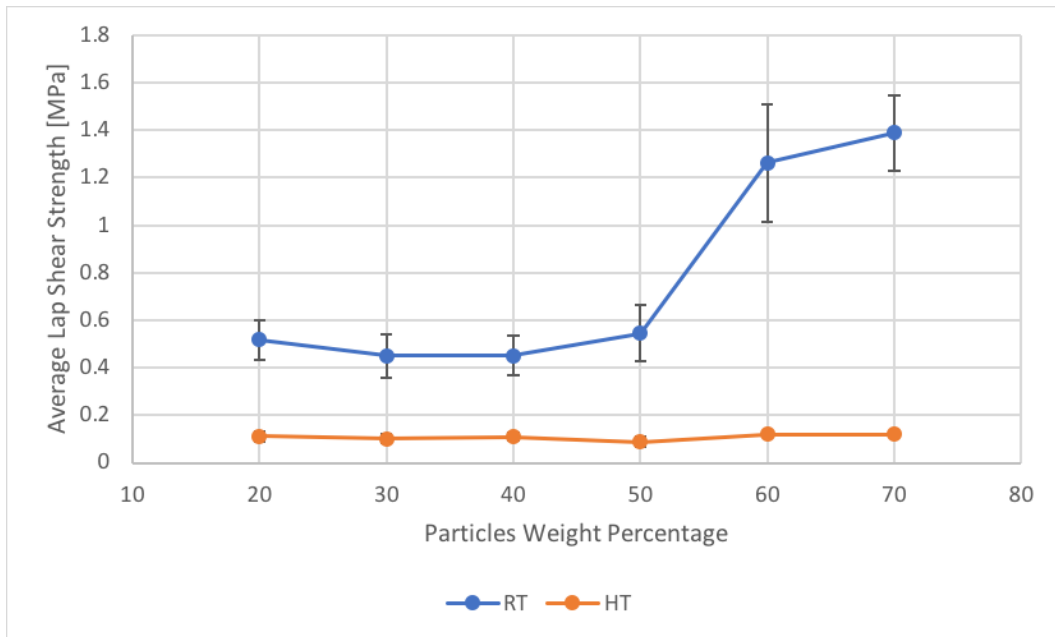


Figure 5.14 - Effect of testing temperature - Cycled Small particles

As it has been noticed for the tests at room temperature, the failure mode that has been observed in all the tests performed at 70 °C was interfacial.

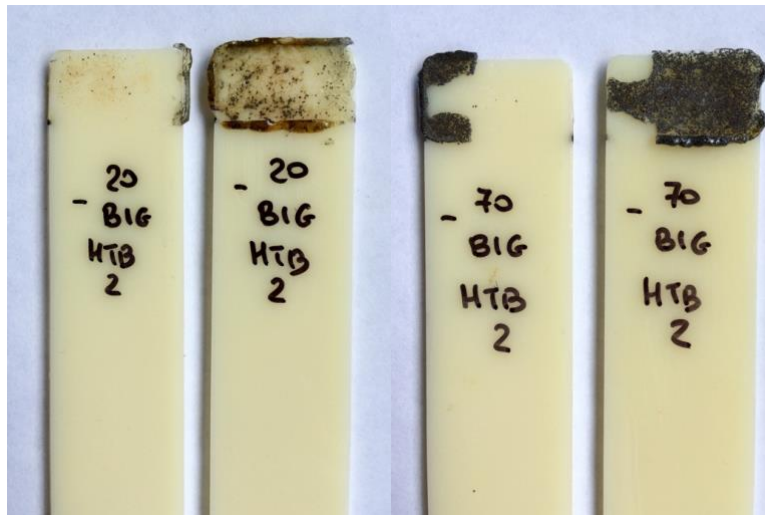


Figure 5.15 - Interfacial failure mode - High Temperature with 20 % (left) and 70 % (right) of “big” particles

5.2 Reversibility performances

The reversibility capabilities of the joints analyzed in this study have been measured with debonding tests. All the combinations of modified hot-melt adhesive in terms of iron particulate sizes and weight percentage that have been observed in this study have been used for these tests. The latter have been performed only on baseline modified HMAs at room temperature. The aim of these experiments is to observe the time that is required to debond the joints by applying the same high frequency electromagnetic field that has been used to bond them in order to melt the polymer matrix.

The results of these debonding tests are summarized in the Fig. 5.16. It can be observed that the time required to debond the specimens decreases with the weight percentage with an almost linear trend.

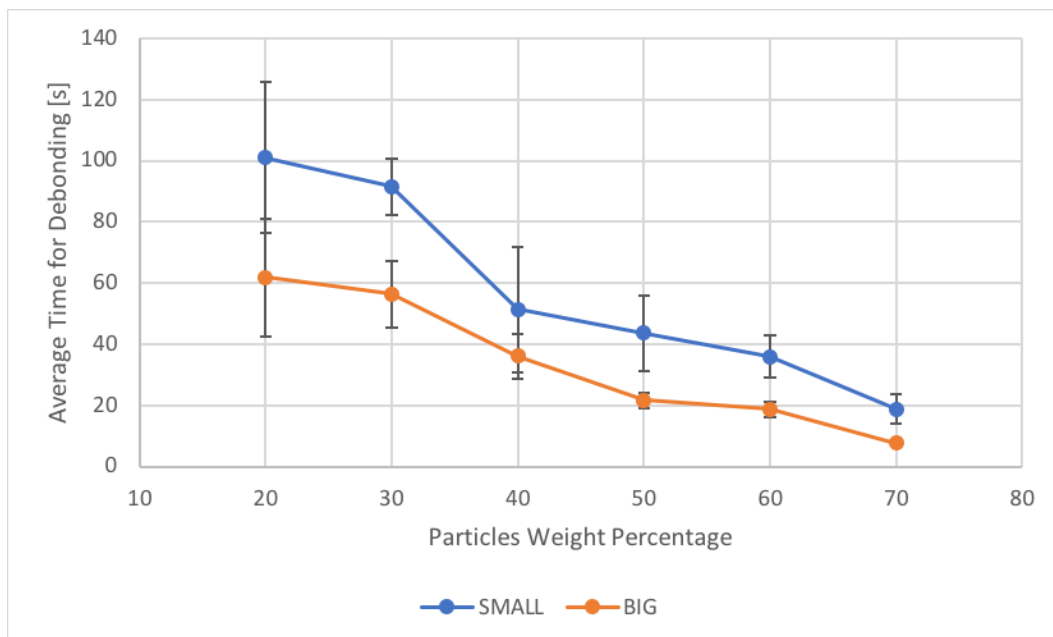


Figure 5.16 - Time required to debond the Single Lap Joints

It can be highlighted that the size of the used particulate influences the measured time with a constantly a smaller number of seconds required to debond the specimens with the bigger iron particles given a fixed weight percentage of metal in the compound.

This result can be linked to the one that has previously been obtained when the time required to obtain a complete melting of the adhesive had been evaluated. The time measured in the debonding tests for each combination of size and weight percentage of iron micro-particles is smaller than the one evaluated in the bonding phase. This happens because, in this test, the presence of weight connected to one of the two halves of the joint represents a constant vertical force of 4.9 N that pulls the sample and that is able to overcome the strength of the joint before all the adhesive is uniformly melted.

It can be observed that the higher is the amount of metal particles in the polymer, the smaller is the time that the modified hot-melt adhesive needs to reach the melting temperature. Moreover, the choice of the particulate size changes the results due to a bigger heat transfer coefficient that the bigger particles have with respect to the smaller one. Therefore, a bigger particles addition may be considered in the case of applications in which the process time is considered a big constrain and a reduction in terms of strength performance can be allowed.

In particular, the lowest measured time has been 7.67 seconds for the single lap joints with 70 % of iron in the bigger particulate size. For the same weight percentage but with the smaller size of micro-particles, a time 18.83 seconds has been observed. On the other hand, the highest measured value is 101 seconds in the case of the specimens with 20 % of smaller particulate size in the polymer. It is worth to notice that this amount of time may be reduced increasing the power of adopted machine. It has been observed that the latter value can be moved to 43 seconds increasing the power from 500 W to 1000 W. These tests with a higher power have not been included in this work because of their unreliability on samples with high percentages of metal

embedded but they highlight the possibility of using a wider range of modified HMA configurations also in situations in which the process time is an issue that has to be overcome.

5.3 DMA tests

The main objective of this study has been the evaluation of the performances in terms of strength and reversibility of single-lap joints manufactured with hot-melt thermoplastic adhesives in which iron particles have been embedded in different particulate sizes and weight percentage. Apart from the quasi-static shear tests performed on the SLJs, a more detailed investigation on the adhesives has been done in order to understand deeply the behavior of the polymer with or without the addition of metal in its matrix. To this purpose, the pristine hot-melt adhesive together with the modified ones in which the 30 % and 60 % of iron micro-particles have been mixed in both the particulate sizes have been subjected to two different tests with the Dynamic Mechanical Analyzer.

The first experiment has had the objective of identifying the response of the materials when subjected to dynamic oscillations to characterize the viscoelastic behavior of the polymer.

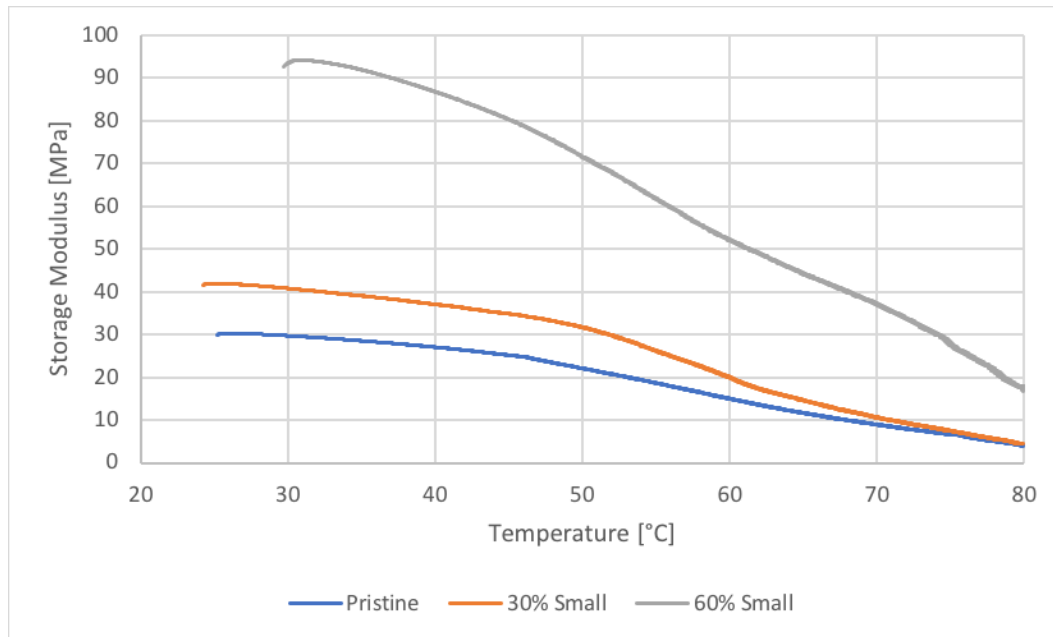


Figure 5.17 - Storage modulus - Effect of weight percentage - Frequency of 1 Hz

In the Figure 5.17 it is shown the trend of the storage modulus in a range of temperature between RT and 80 °C for three different tested adhesives. The blue line is referred to the pristine adhesive while the orange and the grey lines represent the storage moduli of the samples with 30 % and 60 % of small iron particles. It can be observed that the all the three specimens have a value of E' that decreases with the increasing temperature. This means that the stiffness and the shape recovery of the polymer during loading are reduced to values that are less than the 20 % of the ones at room temperature. The reduction of storage modulus agrees with the results obtained in the quasi-static shear tests on the SLJs at high temperature in which the measured LTC has been very low with respect to the RT tests. Therefore, the adhesive shows a very strong dependence on the working temperature. As also previously observed, this represents an important constrain for the application of a similar solution.

It can be observed that the presence of the metal particles in the matrix of the hot-melt adhesive shifts up the storage modulus curves with a factor that depends by the weight percentage of the

iron in the compound. In fact, a relevant amount of metal generates a bigger stiffness with respect to the more ductile pristine adhesive thus increasing the storage modulus.

The effect of the particulate size is shown in the Figure 5.18. Given a constant weight percentage of 60 % of iron micro-particles mixed with the pristine HMA, the same test has been repeated for samples with the bigger size of the particulate. The storage modulus decreases with the increasing temperature as it has been observed in the other tests, but it is reduced of a value that is in a range between the 20 % and the 25 % with respect to the sample with the smaller particles.

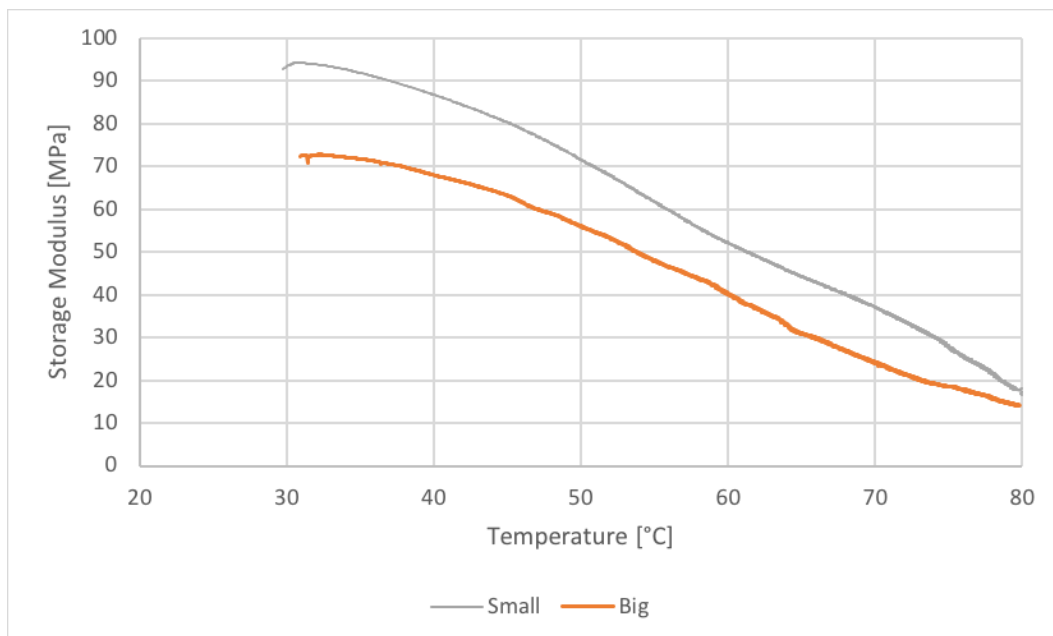


Figure 5.18 - Storage modulus - Effect of particulate size (60 % enrichment) - Frequency of 1 Hz

Another variable that has been investigated is the frequency of the oscillation, that represents an equivalent modification of the strain rate. In the Figure 5.19 is presented a comparison between the results obtained with the same adhesive configuration (HMA modified with 60 % of small particles) tested with an oscillation of the movable clamp having a frequency of 1 Hz and 100 Hz.

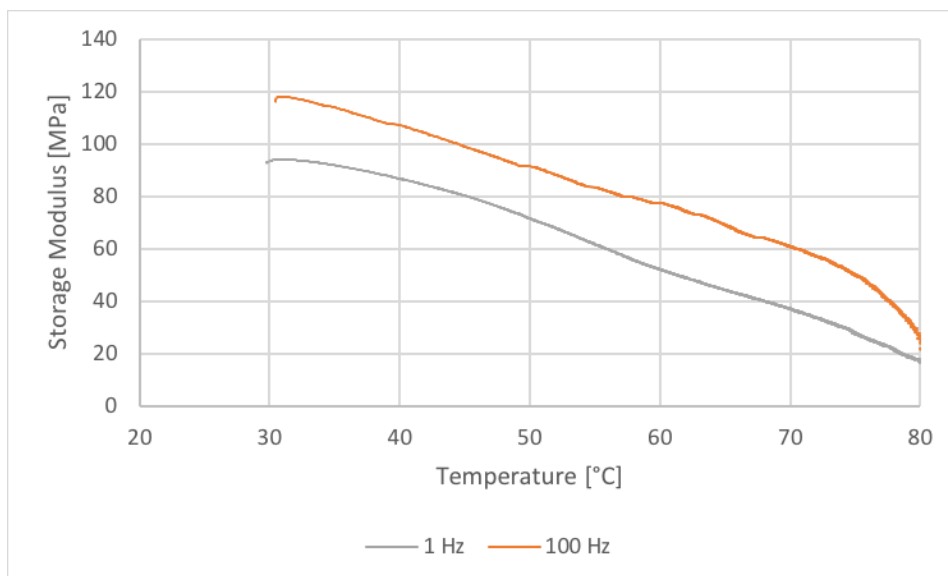


Figure 5.19 - Storage modulus - Effect of frequency - Adhesive with 60 % of smaller particles

The modification of the frequency value from 1 to 100 Hz increases the storage modulus of the samples of a quantity around the 30 %. This phenomenon occurs because the frequency of the oscillation is inversely proportional to the time. This means that at higher frequency there is less time for the molecular relaxation and it is required a higher force to deform the material thus leading to a bigger value of the storage modulus. In particular, the value of E' that the considered sample had at room temperature when tested with a frequency of 1 Hz is again obtained at a temperature of 50 °C when it is subjected to a 100 Hz oscillation.

The same DMA tests have given another important output result such as the loss modulus. It is worth to notice that the dependence with the temperature for E'' is represented by a decreasing curve as it has been observed for the storage modulus. This means that the damping behavior, which indicates the polymer's ability to disperse mechanical energy through internal molecular motions, decreases with the increasing loading temperature of the sample. This result highlights the fact that all the HMAs used for these DMA tests have been observed in a range of temperature that is above the glass-transition temperature of the material. In fact, as temperature

continues to increase above the GTT, molecular frictions are reduced, less energy is dissipated, and the loss modulus decreases. On the other hand, when testing a material under its GTT, the storage modulus decreases, and the loss modulus increases with the increasing temperature, thus leading to a peak in the loss modulus curve in proximity of the glass-transition temperature. As it has happened in the case of the storage modulus, also the E'' increases when iron particles are mixed to the pristine adhesive.

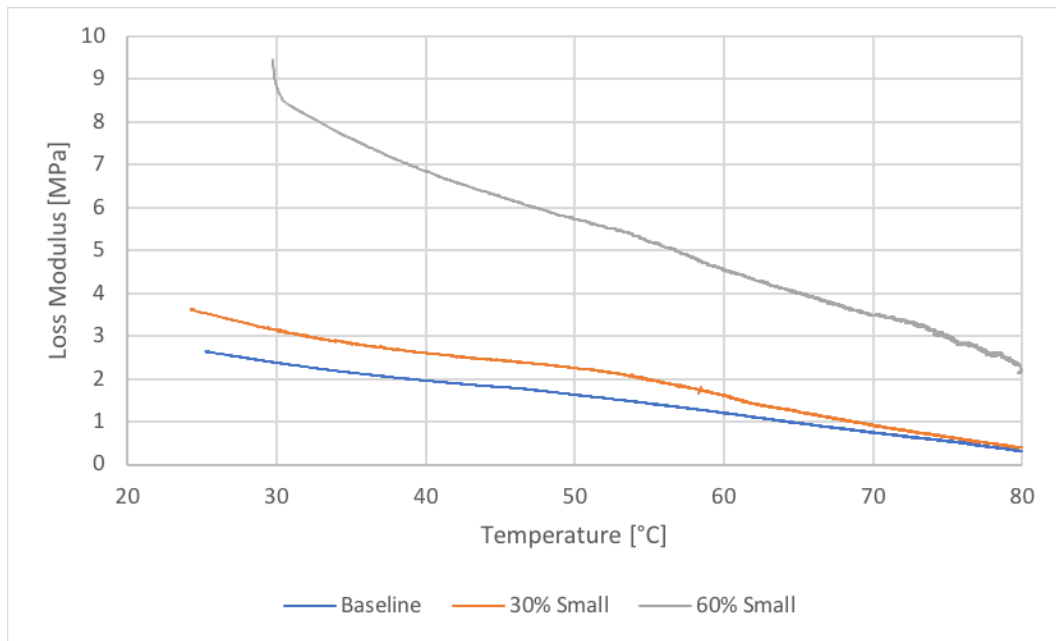


Figure 5.20 - Loss modulus - Effect of particles weight percentage - Frequency of 1 Hz

The particulate size and the frequency of the oscillation have an effect on the loss modulus that is the same that has been measured and explained for the E' .

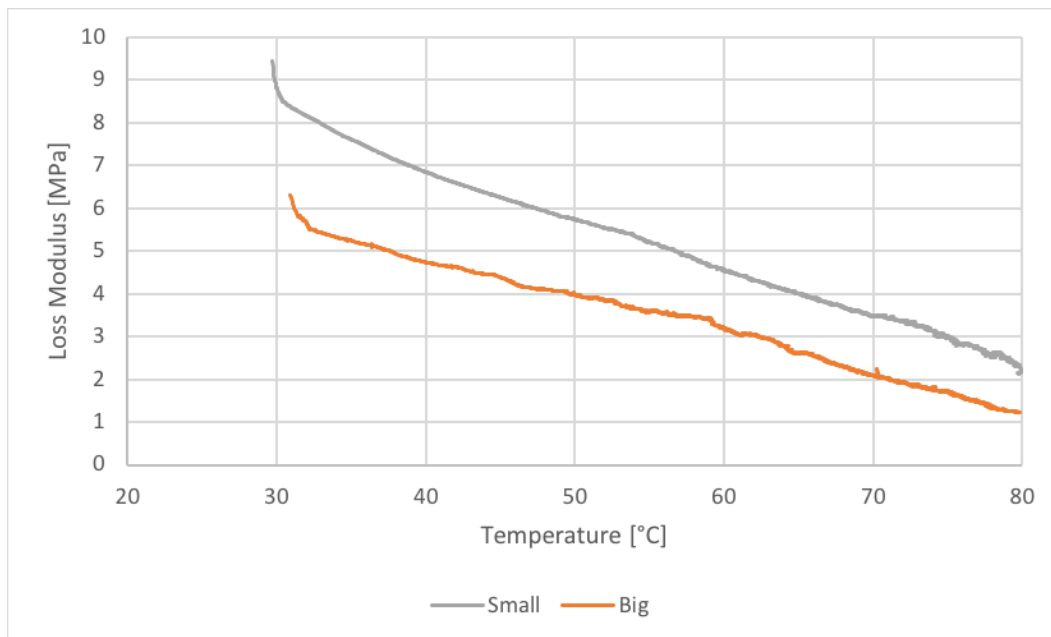


Figure 5.21 - Loss modulus - Effect of particulate size (60 % enrichment) - Frequency of 1 Hz

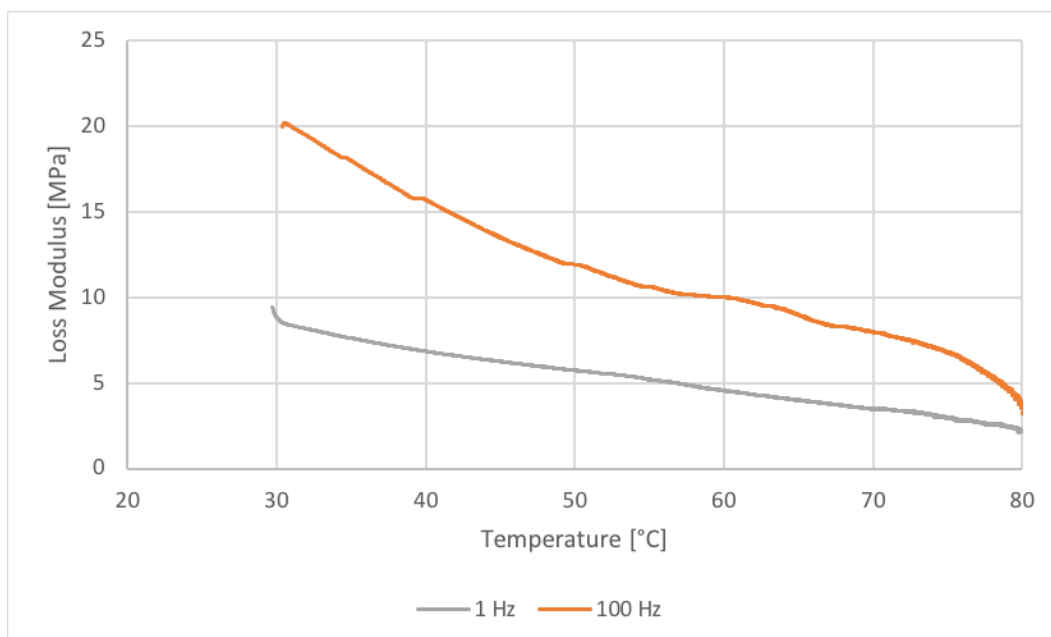


Figure 5.22 - Loss modulus - Effect of frequency - Adhesive with 60 % of small particles

The last quantity that has been measured with the DMA test at constant strain rate is the tangent of the angle δ . This value represents the ratio between the storage modulus E' and the loss

modulus E'' . The angle δ is described the phase difference between the stress and strain sine waves. The value of its correspondent tangent is a sensitive indicator of the thermal/mechanical conditions that cause significant bond rotation or intermolecular friction and flow and determines how much a material is far from being purely elastic or purely viscous.

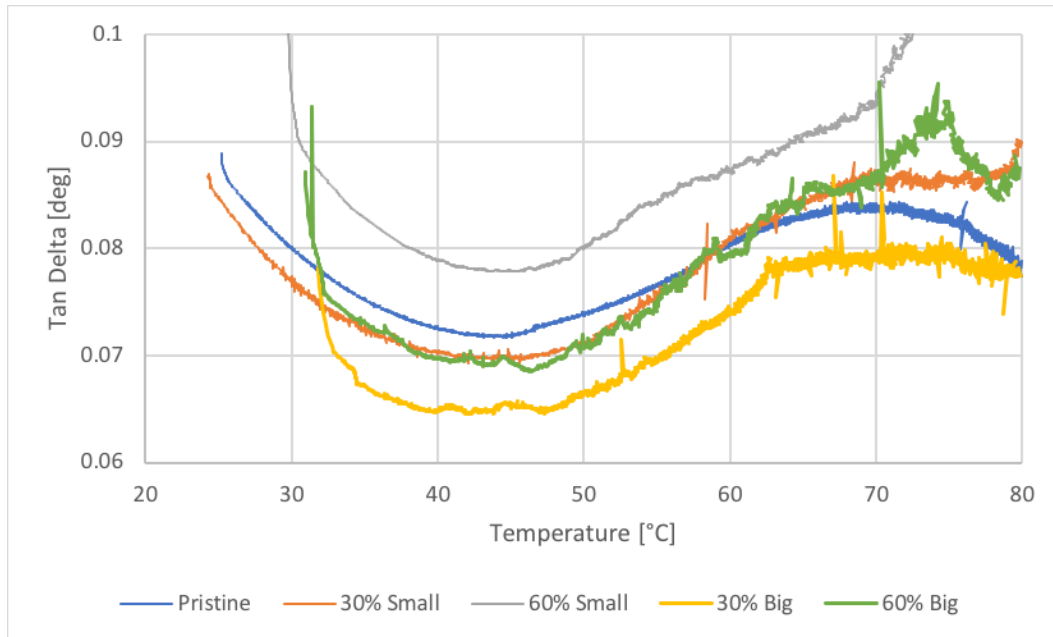


Figure 5.23 - Tan Delta - Effect of adhesive enrichment - Frequency of 1 Hz

The Figure 5.23 shows the $\tan \delta$ that has been measured in the tests with an oscillation frequency of 1 Hz for the five different configurations that have been tested. It can be observed that the trend of this curve is similar between the different combinations of HMA and metal particles. In particular, it is worth to notice that all the curves share a minimum value between the temperature of 43 °C and 45 °C. This observation allows the author to consider the effect of the modification of the pristine adhesive as negligible in terms of variations of the viscoelastic properties of the HMA due to the fact that there is no shift on the horizontal axis that could have represented a modification in the glass-transition temperature of the modified hot-melt adhesive with respect to the pristine one.

The characterization of the properties of the adhesive has been completed with an investigation on the behavior of the HMA subjected to quasi-static tensile tests that have led to the load vs. displacement curve of the different adhesive combinations. Tests have been performed with the DMA testing machine at room temperature and at 70 °C.

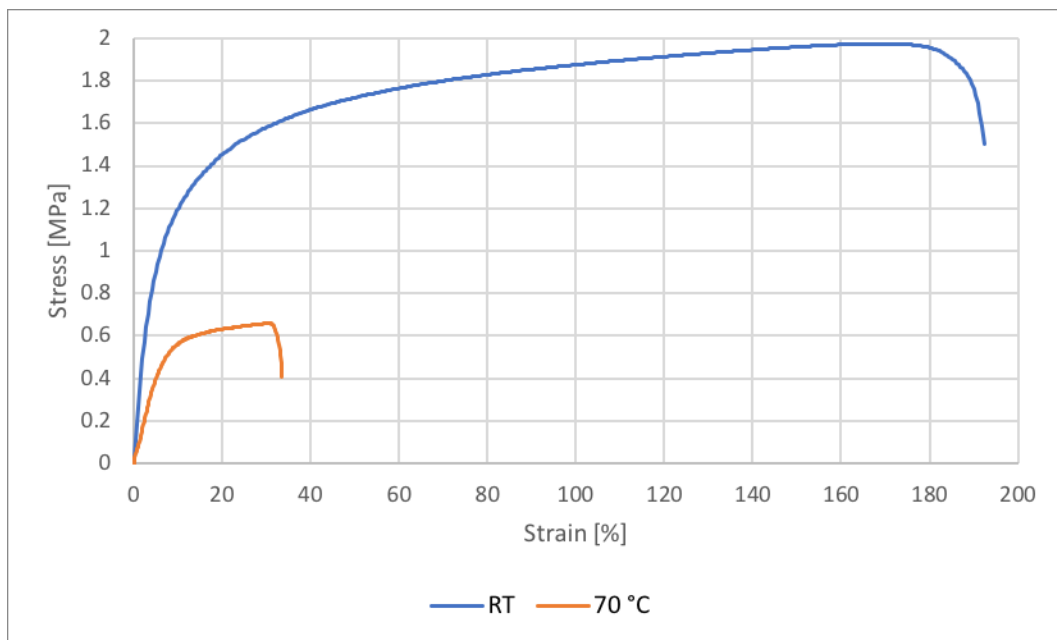


Figure 5.24 - Quasi-static tensile test - Effect of testing temperature - Pristine adhesive

The pristine adhesive has shown an elongation at break of 192 % and a value of maximum stress equal to 1.97 MPa. In the Figure 5.19 it can be observed the effect of the testing temperature on the pristine adhesive. The behavior that has been measured on the sample pulled at 70 °C highlights a relevant reduction in both ductility and mechanical strength. In this case, the elongation at break has been 33.6 % and the maximum stress equal to 0.66 MPa. Moreover, a reduction of the Young's modulus is measured. Its value has been reduced from 21.4 MPa to 8.38 MPa meaning that the material has a lower stiffness at higher temperature and that its resistance to recover the original shape after an elastic deformation is reduced.

The addition of iron micro-particles has also an important effect on the load vs. displacement curve of the hot-melt adhesive. The Figure 5.25 shows a comparison between the results obtained at room temperature with the pristine and the modified adhesive. The modified samples that have been considered are the one in which the 30 % and the 60 % of iron particles in the smaller size are embedded.

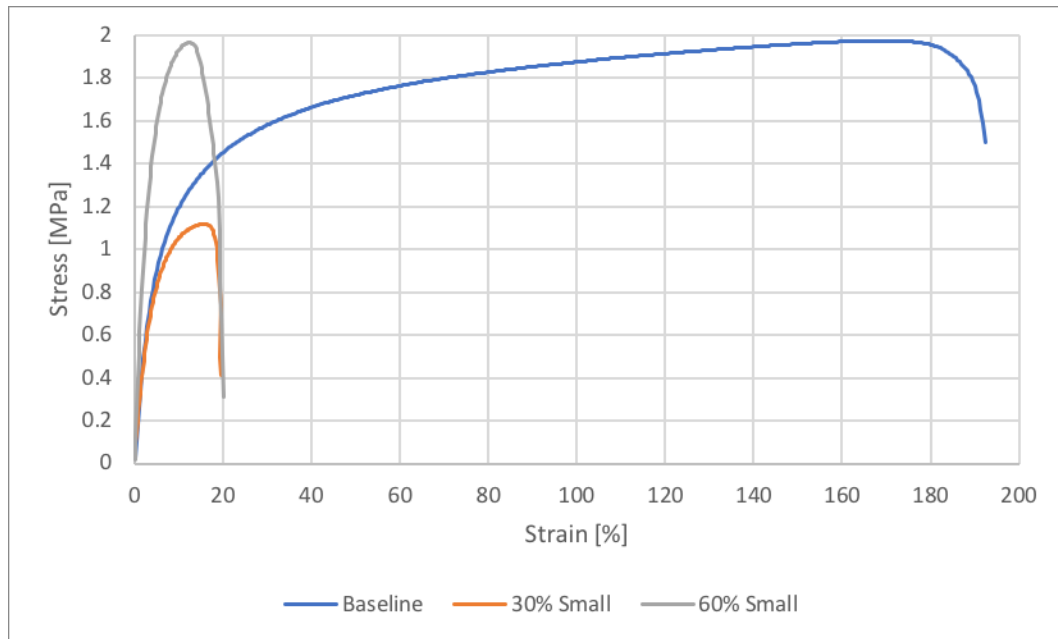


Figure 5.25 - Quasi-static tensile test - Effect of enrichment level - Room Temperature

It can be observed that the presence of the metal in the polymer matrix modifies the ductility of the sample so that the elongation at break for the specimens with the mixed particles has been reduced to a value of 20 %. The maximum stress that has been measured for the sample with the 60 % of particles is 1.96 MPa, a value that is almost the same of what it has been obtained for the pristine adhesive. The HMA with the 30 % of iron embedded has given a result of 1.12 MPa. The effect of the particulate size can be observed observing a comparison between the adhesives with 30 % of iron in the two dimensions of particulate. The reference value is given by the pristine adhesive. It is possible to notice that the ductility is higher for the samples with

the bigger particles mixed into the adhesive matrix. The correspondent elongation at break is equal to 69 % and the ultimate strength is 1.47 MPa.

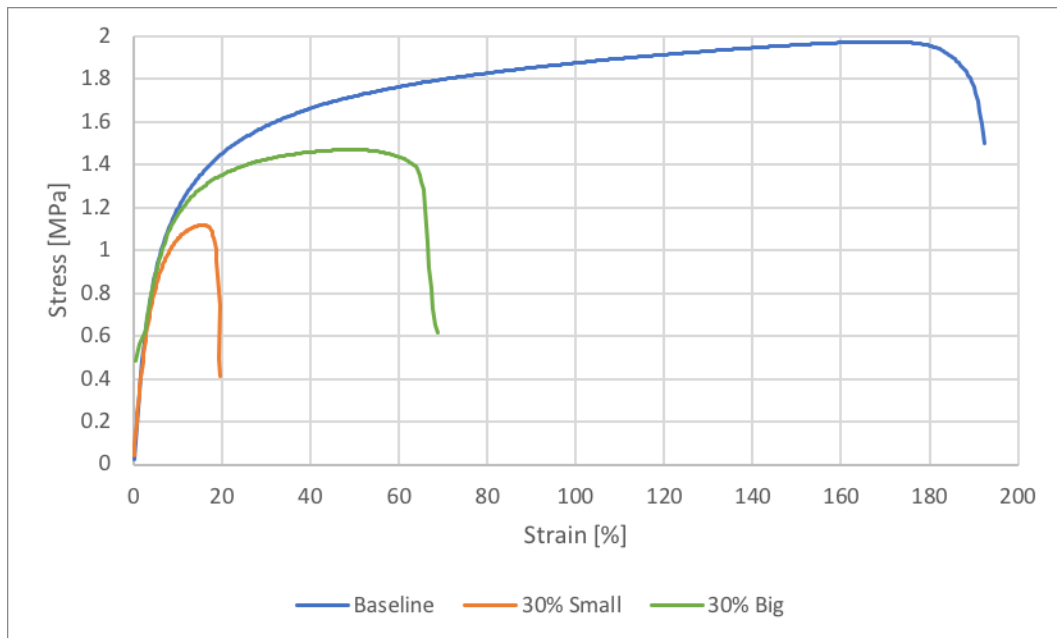


Figure 5.26 - Quasi-static tensile test - Effect of particulate size - Room Temperature

A further observation can be done by observing the Young's modulus. For the two samples with the 30 % of iron micro-particles, the correspondent measured moduli have been 20.43 MPa and 20.84 MPa, that are values close to the pristine adhesive's one. On the other hand, the specimen with the 60 % of small iron particulate has given a result of 38.99 MPa for the Young's modulus. This so big increase of stiffness may be linked to the amount of metal in the overall mass of the modified HMA. A so high weight percentage of iron inside the polymer matrix may start a modification in the overall behavior of the material thus hiding the mechanical characteristics of the pristine adhesive and showing a more stiff, brittle and metal-like load vs. displacement curve.

6 **Conclusions**

This study provides an insight into the characterization of the mechanical behavior of adhesive SLJs made of ABS adherends bonded with an HMA enriched with iron micro-particles. The main objective of the work is the analysis of the effects of the weight percentage and size of the added particulate on the mechanical performance and reversibility capability of the joints.

The quasi-static shear tests highlighted values of lap-shear strength for an average level of enrichment that are reduced with respect to the pristine adhesive. Specimens with higher weight percentages of particles gave results of LTC that reached values bigger than the reference ones, due to mechanical friction and micro-welding among particles. Environmental cycling reduced the joints strength due to the harmful presence of moisture inside the polymer that affected the HMA both in the pristine and in the modified configurations.

The testing temperature had an important consequence on all the observed specimens. Tests performed at 70 °C showed a dramatic drop in the mechanical performances. This result is identified as the main drawback of this bonding solution and represents an important constrain in possible industrial applications.

For the all quasi-static shear tests performed, the bigger particulate gave lower performances in terms of mechanical strength. On the other side, faster processing and debonding times were measured due to the higher heat transfer coefficient of the larger particles.

Debonding tests were performed on the joints at room temperature without exposure to environmental cycling. The trend of the results followed the one observed during the manufacturing of the joints with a reduction of time with the increasing weight percentage of the iron particles. All the tested samples fractured with interfacial failure mode.

DMA tests gave results on the dynamic and static mechanical performances of the HMA in its pristine and enriched (30 % and 60 % of particles) configurations. Reductions of both storage and loss moduli were noticed with the increasing temperature for all the specimens thus meaning a lower stiffness, less ability to recover shape and to disperse mechanical energy of the polymer during loading at higher temperature. The measured values of the tangent of the angle δ showed that the enrichment of the HMA does not modify the effect of temperature on the viscoelastic properties of the adhesive showing curves that share the minimum values at the same temperature and show the same trend in all the observed range.

The quasi-static tensile tests performed with the DMA machine highlighted a reduction of ductility of the polymer due to the presence of iron micro-particles and confirmed the dramatic worsening effect of the loading temperature on the mechanical performances of the HMA that were observed in the shear tests on the SLJs.

Bibliography

- [1] Pozar, D.M., “Microwave Engineering Addison”, 1993, 1st Ed., Wesley Publishing Company, Boston
- [2] Galindo, B., Benedito, A., Ramos, F., Gimenez, E., “Microwave Heating of Polymers: influence of carbon nanotubes dispersion on the microwaves susceptor effectiveness”, 2013, 6th International Conference on Carbon Nanoparticle Based Composites, Dresden
- [3] Neto, A.C., Guinea, F., Peres, N.M., “Drawing conclusions from graphene”, 2006, Phys. World, vol. 19, n. 11, pp. 33-37
- [4] Kulekci, M.K., “Magnesium and its alloys application in automotive industry”, 2009, International Journal Advanced Manufactory Technology, pp. 851-865
- [5] Lu, Y., Broughton, J., Winfield, P., “A review of innovations in disbonding techniques for repair and recycling of automotive vehicles”, 2014, International Journal of Adhesion & Adhesives 50, pp. 119-127
- [6] Ciardiello, R., “Functionalization of adhesives and composite matrix by micro and nanoparticle addition”, 2018, Politecnico di Torino, PhD Thesis
- [7] Verna, E., Cannavaro, I., Brunella, V., Koricho, E.G., Belingardi, G., Roncato, D., Martorana, B., Lambertini, V., Neamtu, V.A., Ciobanu, R., “Adhesive joining technologies activated by electro-magnetic external trims”, 2013, International Journal of Adhesion & Adhesives 46, pp. 21-25

- [8] Banea, M.D., Da Silva, L.F.M., Carbas, R.J.C., “Debonding on command fro adhesive joints for the automotive industry”, 2015, International Journal of Adhesion & Adhesives 59, pp. 14-20
- [9] Grewell, D.A., Benatar, A., Park, J.B., “Plastic and Composites Welding Handbook”, Munich, Hanser Publishers, pp. 110-112
- [10] Cagle, C.V., “Handbook of Adhesive Bonding”, 1973, United States, McGraw-Hill
- [11] Li, W., Bouzidi, L., Narine, S.S., “Industrial and Engineering Chemistry Research”, 2008, Vol. 47, pp. 7524-7532
- [12] Koricho, E., “Implementation of composites and plastic materials for vehicle lightweight”, 2012, Politecnico di Torino, PhD Thesis
- [13] Tremblay, S., “Advances in Hot Melt Technology Yield High Performance Structural”
- [14] Gil, P.R., Loretta, L., Del Pino, P., Javier, A.M., Parak, W.J., “Nanoparticle-modified polyelectrolyte capsules”, 2008, NanoToday, pp. 12-21
- [15] Skirtach, A.G., Javier, A.M., Kreft, O., Kohler, K., Alberola, A.P., Mohwald, H., Parak, W.J., Sukhorukov, G.B., “Laser-induced Release of Encapsulated Materials inside Living Cells”, 2006, Chem. Int. Ed (42), pp. 4612-4617
- [16] Skirtach, A.G., Dejugnat, C., Braun, D., Sussha, A.S., Rogach, A.L., Parak, W.J., Mohwald, H., Sukhorukov, G.B., “The Role of Metal Nano-particles in remote release of encapsulated materials”, 2005, Nano Lett. (5), pp. 1371-1377
- [17] Boucharda, L.S., Sabieh Anwarb, M., Gang, L., Hanne, B., Xied, Z.H., Grayc, J.W., Wange, X., Pinesf, A., Chenc, F.F., “Picomolar sensitivity MRI and photoacoustic imaging of cobalt nano-particles”, 2009, PNAS, vol. 106 (11), pp. 4085-4089

- [18] “Annual Book of ASTM Standards”, volume 15.06
- [19] <http://mtskorea.com/2012/kr/products/producttype/test-components/environmental-simulation/chambers/index.htm>
- [20] https://www.engineeringtoolbox.com/dry-air-properties-d_973.html
- [21] <https://multimedia.3m.com/mws/media/104313O/3mtm-epoxy-and-hot-melt-adhesives-for-electronics.pdf>
- [22] <https://plastics.ulprospector.com/generics/1/c/t/acrylonitrile-butadiene-styrene-abs-properties-processing>
- [23] <http://www.cintestlabs.com/services/thermal-properties>
- [24] DMA Q800 User Manual, TA Instruments
- [25] Dunson, D., “Characterization of polymers using Dynamic Mechanical Analysis (DMA)”, 2017, EAG
- [26] http://www.lamieux.asia/fileadmin/content/bilder/protect/hotmelt-moulding/verbrauchsmaterial/TDS_EN_-_THERMELT_865_Natural_03-2015.pdf
- [27] <http://www.matweb.com/search/datasheettext.aspx?matguid=b3744ecb6a1741898d35ea92b14140e7>